A regional air quality forecasting system over Europe: the MACC-II daily ensemble production

V. Marécal[1], V.-H. Peuch[2], C. Andersson[3], S. Andersson[3,] J. Arteta[1], M. Beekmann[4], A. Benedictow[5], R. Bergström[3], B. Bessagnet[6], A. Cansado[7], F. Chéroux[1], A. Colette[6], A. Coman[4], R. L. Curier[8], H. A. C. Denier van der Gon[8], A. Drouin[1], H. Elbern[9], E. Emili[10], R. J. Engelen[2], H. J. Eskes[11], G. Foret[4], E. Friese[9], M. Gauss[5], C. Giannaros[12], J. Guth[1], M. Joly[1], E. Jaumouillé[10], B. Josse[1], N. Kadygrov[1], J. W. Kaiser[13], K. Krajsek[14], J. Kuenen[8], U. Kumar[11], N. Liora[12], E. Lopez[7], L. Malherbe[6], I. Martinez[7], D. Melas[12], F. Meleux[6], L. Menut[15], P. Moinat[10], T. Morales[7], J. Parmentier[1], A. Piacentini[10], M. Plu[1], A. Poupkou[12], S. Queguiner[1], L. Robertson[3], L. Rouïl[6], M. Schaap[8], A. Segers[8], M. Sofiev[16], L. Tarasson[17], M. Thomas[3], R. Timmermans[8], Á. Valdebenito[5], P. van Velthoven[11], R. van Versendaal[11], J. Vira[16] and A. Ung[6]

[1] {Groupe d'étude de l'Atmosphère Météorologique/Centre National de Recherches Météorologiques, CNRS-Météo-France, UMR 3589, Toulouse, France}

[2] {European Centre for Medium-range Weather Forecasts, Reading, UK}

[3] {Swedish Meteorological and Hydrological Institute, Norrköping, Sweden}

[4] {Laboratoire Inter-universitaire des Systèmes Atmosphériques, UMR CNRS 7583, Université Paris Est Créteil et Université Paris Diderot, Créteil, France}

[5] {Norwegian Meteorological Institute, Oslo, Norway}

[6] {Institut National de l'Environnement Industriel et des Risques, Parc Technologique Alata, 60550 Verneuil en Halatte, France}

[7] {AEMET Spanish Meteorological State Agency, Leonardo Prieto Castro 8, 28040, Spain}

[8] {TNO, Climate Air and Sustainabilty Unit, Utrecht, The Netherlands}

[9] {Rhenish Institute for Environmental Research at the University of Cologne, Cologne, Germany}

[10] {CERFACS, URA 1875, Toulouse, France}

[11] {Royal Netherlands Meteorological Institute, De Bilt, The Netherlands}

[12] {Laboratory Of Atmospheric Physics, Physics Dept., Aristotle University of Thessaloniki, Thessaloniki, Greece}

[13] {Max Planck Institute for Chemistry, Mainz, Germany}

[14] {Institut für Energie- und Klimaforschung (IEK-8), Forschungszentrum Jülich, Jülich, Germany}

[15] {Laboratoire de Météorologie Dynamique, Ecole Polytechnique, 91128 Palaiseau, France}

[16] {Finnish Meteorological Institute, Erik Palmenin Aukio 1, Helsinki 00560, Finland}

[17] {Norwegian Institute for Air Research, 2027 Kjeller, Norway}

Correspondence to: Virginie Marécal (virginie.marecal@meteo.fr)

Abstract

This paper describes the pre-operational analysis and forecasting system developed during MACC (Monitoring Atmospheric Composition and Climate) and continued in MACC-II (Monitoring Atmospheric Composition and Climate: Interim Implementation) European projects to provide air quality services for the European continent. This system is based on seven state-of-the art models developed and run in Europe (CHIMERE, EMEP, EURAD-IM, LOTOS-EUROS, MATCH, MOCAGE and SILAM). These models are used to calculate multi-model ensemble products. The paper gives an overall picture of its status at the end of MACC-II (summer 2014) and analyses the performance of the multi-model ensemble. The MACC-II system provides daily 96h forecasts with hourly outputs of 10 chemical species/aerosols (O_3, NO_2, SO_2, CO, PM_{10}, $PM_{2.5}$, NO, NH_3, total NMVOCs and PAN+PAN precursors) over 8 vertical levels from the surface to 5km height. The hourly analysis at the surface is done *a posteriori* for the past day using a selection of representative air quality data from European monitoring stations.

The performance of the system is assessed daily, weekly and 3 monthly (seasonally) through statistical indicators calculated using the available representative air quality data from European monitoring stations. Results for a case study show the ability of the ensemble median to forecast regional ozone pollution events. The seasonal performances of the individual models and of the multi-model ensemble have been monitored since September 2009 for ozone, NO_2 and PM_{10}. The statistical indicators for ozone in summer 2014 show that

the ensemble median gives best performances on average compared to the seven models. There is very little degradation of the scores with the forecast day but there is a marked diurnal cycle, similarly to the individual models, that can be related partly to the prescribed diurnal variations of anthropogenic emissions in the models. During summer 2014, the diurnal ozone maximum is underestimated by the ensemble median by about 4 μg m^{-3} on average. Locally, during the studied ozone episodes, the maxima from the ensemble median are often lower than observations by 30 to 50 μg m^{-3}. Overall, ozone scores are generally good with average values for the normalized indicators of 0.14 for the Modified Normalized Mean Bias and of 0.30 for the Fractional Gross Error. Tests have also shown that the ensemble median is robust to reduction of ensemble size by one, that is if predictions are unavailable from one model. Scores are also discussed for PM_{10} for winter 2013-1014. There is an underestimation of most models leading for the ensemble median to a Mean Bias of -4.5 μg m^{-3}. The ensemble median Fractional Gross Error is larger for PM_{10} (~0.52) than for ozone and the correlation is lower (~0.35 for PM_{10} and ~0.54 for ozone). This is related to a larger spread of the 7 model scores for PM_{10} than for ozone linked to different levels of complexity of aerosol representation in the individual models. In parallel, a scientific analysis of the results of the seven models and of the ensemble is also done over the Mediterranean area because of the specificity of its meteorology and emissions.

The system is robust in terms of the production availability. Major efforts have been done in MACC-II towards the operationalisation of all its components. Foreseen developments and research for improving its performances are discussed in the conclusion.

1. Introduction

The chemical composition of the air close to the Earth's surface, generally referred as 'air quality' (AQ), directly affects human and animal health and also the vegetation. For instance, ozone has a known impact on the respiratory system (e.g. WHO, 2004) and on the vegetation development (e.g. Fuhrer and Booker, 2003). Recently, the World Health Organisation reported that in 2012 around 3.7 million people deaths are attributable to ambient air pollution (http://www.who.int/phe/health_topics/outdoorair/databases/en/). This is why air quality has become a major concern, starting in the 1970's, in particular in Europe (e.g. WHO, 2013). Since the Helsinki Protocol in 1985, many regions and countries, including the European Union countries, have progressively put in place tools to regulate and to control the emissions

of the main air pollutants. This has led to an important effort to monitor the air composition near the surface but also to develop air quality forecasting systems in experimental or operational modes (see reviews by Ebel et al. 2005, Menut and Bessagnet 2010). These tools can be used in cases of high pollution episodes to inform people and to take emergency measures to prevent harming effects. They can also be used for policy makers for the regulations on air pollutant emissions and for monitoring the effect of these regulations on air quality (episodes and also background pollution).

The main pollutants under focus for air quality are ozone, nitrogen oxides (NOx= NO_2 + NO), sulphur dioxide (SO_2), Volatile Organic Compounds (VOCs), ammonia (NH_3), particulate matter, heavy metals (Pb, Cd, Hg) and Persistent Organic Pollutants (POPs, e.g. pesticides and dioxine). Ozone is a secondary pollutant meaning that it is not emitted but produced from gaseous precursors (mainly VOCs and NOx) originating from both natural and anthropogenic sources. Particulate matter (PM) corresponds to small size aerosols. PMs are categorised as PM_{10} (size < 10 μm), $PM_{2.5}$ (size < 2.5 μm) and PM_1 (size < 1 μm). These categories were chosen because of their known effects on health. In PMs, the distinction between primary (dust, sea salts, black carbon and organic carbon) and secondary aerosols formed from gaseous precursors such as SO_2, DMS, H_2S, NH_3, NOx and VOCs is ignored when considering mass or number concentration only.

Besides the development of surface measurement networks for these main pollutants, there has been a sustained research effort on the atmospheric chemistry modelling for air quality forecasting purposes. Regional and local air quality forecasting systems (Kukkonen et al. 2012; Zhang et al., 2012) rely on limited area models that can be based either on an off-line or an on-line approach to take into account the effect of meteorological conditions on air composition. Off-line chemistry models, known as Chemistry Transport Models (CTMs), use the meteorological parameters from the analyses or the forecasts provided by a separate numerical weather prediction model. On-line models are meteorological models in which chemical variables and processes are included (Baklanov et al., 2014). On-line models have the capability to represent the feedback of the chemical composition on meteorological parameters but they are computationally demanding by design. This is why CTMs are generally preferred for operational air quality forecasting systems.

The chemical composition of air depends on many processes that need to be well represented in models in order to provide reliable air quality forecasts (e.g. Rao et al. 2011). The composition near the surface is very much driven by emissions but also by chemical processes

(gaseous/heterogeneous reactions and photolysis) including the production of secondary pollutants, by the advection by winds, by the diffusion in the planetary boundary layer, by the scavenging by rain and by the dry deposition at the surface. Each of these processes has its own uncertainty. These uncertainties come, on one hand, from the limit of our current knowledge and, on the other hand, from the need to simplify the process representation in models because of computational constraints. In meteorology and climate studies, and more recently in atmospheric dispersion and chemistry modelling, the approach based on a multi-model ensemble of forecasts has been developed to provide better information by combining information from different models. The methods vary from very simple such as the average or the median to more elaborated such as weighted averages based on past scores or Bayesian models or spectral methods (e.g. Delle Monache 2006, Riccio et al. 2007, Potempski et al. 2010, Galmarini et al. 2013).

The European Union is very much involved in air quality issues not only through a series of protocols on emissions and consecutive political actions but also by supporting research activities aiming at developing tools for air quality monitoring for Europe. These activities were initiated in the GEMS (Global and regional Earth-system (Atmosphere) Monitoring using Satellite and in-situ data, FP6, 2005-2009, Hollingworth et al. 2008) and PROMOTE (ESA PROtocol MOniToring for the GMES Service Element: Atmosphere, 2006-2009, http://www.gse-promote.org/**)** projects and pursued in the MACC (Monitoring Atmospheric Composition and Climate, FP7, 2009-2011), MACC-II (Monitoring Atmospheric Composition and Climate: Interim Implementation, FP7, 2011-2014) and MACC-III (Monitoring Atmospheric Composition and Climate-III, H2020, 2014-2015) projects. One of the major achievements accomplished in GMES, MACC and MACC-II for European AQ objectives is the development and the exploitation of a pre-operational analysis and forecasting system run on a daily basis. This system is based on the combined use of an ensemble of 7 air quality models. The general objective of this system is not to provide air quality forecasts and analyses for precise local situations but at the pan-European scale. For this purpose, the horizontal resolution chosen for the individual models is between 10 and 20 km, thereby representing large scale phenomena and background air pollution. GEMS involved 10 research and operational models. Evolving towards a pre-operational system, the MACC/MACC-II/MACC-III ensemble is, since 2009, based on seven following state-of-the-art regional CTMs that are all developed and run in Europe and that have been extensively evaluated: CHIMERE (Menut et al., 2013a), EMEP (MSC-W version) (Simpson et al., 2012),

EURAD-IM (Haas et al., 1995; Memmesheimer et al., 2004), LOTOS-EUROS (Schaap et al., 2008), MATCH (Robertson et al., 1999; Andersson et al., 2015), MOCAGE (Josse et al., 2004; Dufour et al., 2004) and SILAM (Sofiev et al., 2008). They are used to produce a multi-model ensemble for major monitored pollutants. Although each of these models can perform very well on particular days in particular areas, the ensemble approach aims at providing on average forecasts and analyses of better quality than any of the individual. It also gives an indication of the uncertainties through the spread between the models. Similarly to meteorological forecasts, the quality of the AQ forecasts needs to be routinely evaluated to provide information to users on its reliability. The performance of the individual and ensemble forecast products is evaluated on a daily basis from comparisons with available surface observations by the European AQ station network. Additionally the system has been providing birch pollen forecasts at surface during the pollen season since 2013. All the forecast and analysis numerical data are publicly available.

The objectives of the paper are, firstly, to provide a description of the pre-operational analysis and forecasting system in place within MACC and MACC-II to provide AQ services for the European continent and, secondly, to document and analyse the performance of the multi-model ensemble. Since the system continuously evolves with time, we present here the configuration at the end of the MACC-II project (summer 2014) with a brief description of recent upgrades included before the end of 2014. An overview of the analysis and forecasting system, including the seven models and the Ensemble, is provided in Section 2. Section 3 is devoted to the system performance for case studies and on a seasonal basis. Section 4 gives a summary and the perspective on short and mid-term developments of the MACC-II system and associated research.

2. Description of the analysis and forecasting systems

2.1 General description of the system

The MACC-II air quality system aims at providing analyses and forecasts of the main pollutants at the regional scale over the European continent: from 25°W to 45°E and from 30°N to 70°N. Each of the 7 models is run at its own horizontal and vertical resolutions, with the horizontal resolutions varying between ~20 km and ~10 km. This range of resolutions is not designed to reproduce local aspects of air pollution but to provide concentrations of pollutants at the regional scale that can then be used in particular as boundary conditions for AQ forecasts at finer resolution.

The range of the forecasts is 96h from 00 UTC on Day0 with hourly outputs on 8 vertical levels (surface, 50m, 250m, 500m, 1000m, 2000m, 3000m and 5000m). Day0 is defined as the day when the forecast is run. The forecast initial time/date is Day0 at 00UTC and final time/date is Day3 at 24UTC. For each timestep (one hour), the individual model fields are interpolated on these vertical levels and on the same regular 0.1° latitude by 0.1° longitude grid over the MACC-II European domain. It is from these re-gridded fields that the ensemble median and verification products are calculated. Before mid-May 2014, only surface, 500m, 1000m and 3000m were produced. The forecast species include O_3, NO_2, SO_2, CO, PM_{10} and $PM_{2.5}$, which are called core species hereafter. The core species are monitored in Near Real-Time (NRT) by European air quality stations and forecasts can therefore be evaluated routinely against these observations. Forecasts of birch pollen concentrations at surface are also produced during the pollen season (1st of March to 30th of June) since 2013. This product is not discussed in this paper since its description and validation is detailed in Sofiev et al. (2015). Additionally, since mid-May 2014, the production has been extended to other species or aggregation of species (NO, NH_3, PAN+PAN precursors, total Non-Methane Volatile Organic Compounds). Additional species are provided primarily for the use as initial and/or boundary conditions mainly for finer scale models designed for local AQ purposes.

The analysis at the surface for Day0-1 is run daily *a posteriori* on Day0 using the assimilation of the hourly data from the AQ monitoring stations available in Europe between 00UTC and 23UTC on Day0-1. Like for the forecasts, Day0 is defined as the day when the analysis is run. Day0-1 refers to the day before Day0. The analysis initial time/date is Day0-1 at 00UTC and final time/date is Day0-1 at 23UTC. Similarly to the forecasts, the hourly individual model fields are interpolated on the same 0.1° latitude by 0.1° longitude grid. The analyses are only produced at the surface level.

Table 1 gives the portfolio of the regional data products. All the additional species and vertical levels are not yet available from all models but this is planned to be completed in 2015. Table 2 gives the current times of delivery of the ensemble numerical data products. These production times have been shifted earlier since summer 2014 in order to fulfil users' needs, in particular Day0 and Day1 forecasts, that are the mostly used products, are now available at 07UTC. This has been made possible by an earlier delivery of the forecasts of each of the 7 models and by replacing the bulk 96h processing of the ensemble by a processing 24 h segments. The delivery time of the analysis has also been shifted earlier in June 2014.

The NRT hourly observations of O_3, NO_2, SO_2, CO, PM_{10} and $PM_{2.5}$ from the European AQ monitoring stations are used for model assimilation to produce the daily analyses and also for the forecast and analysis evaluation. From 2009 until recently, they were gathered country by country through bilateral agreements with the project. Since 2014, a new system has been put in place to gather these observations from the centralised Airbase database maintained by the European Environment Agency (EEA). The database collects the NRT data and validated data from the European countries bound under Decision 97/101/EC to engage in a reciprocal exchange of information (EoI) on ambient air quality. The delivery time of the observations to EEA takes place earlier and there is on average more data available than when gathering them bilaterally country by country, although there is a large variability from one day to another in the number of data available. For the use in the production of the analyses, we chose after a dataflow monitoring of the EEA database a cut-off time at 07 UTC on Day0 for the dataset covering Day0-1. At this time of the day, more than 90% (on average) of all data are available. The 07 UTC cut-off time is therefore a compromise between having enough data available for the model assimilation and a reasonable production time for the ensemble analysis that was at 14:30UTC at the end of MACC-II. This production time is still too late for the forecasts to be initialised from the analysis, meaning that the forecast and the analysis products are currently run in two separate chains for each model. For the product evaluation, the observations covering Day0-1 available in the EEA database at 23UTC on Day0 are used since there is less constraint on the time of delivery of evaluation products. On average there is about 10% more data available at 23UTC than at 07 UTC. As shown in a MACC-II report (D16_3; http://www.gmes-atmosphere.eu/documents/maccii/deliverables/obs/), the additional data collected at 23UTC compared to 07UTC are mainly data from the end of the previous day. This is because there is a significant number of stations that do not send their late afternoon and evening Day0-1 data before 07UTC on Day0. This means that the 23UTC dataset used for verification is homogeneous with approximately the same number of observations in the morning, afternoon and evening.

Because the NRT AQ observations used are not validated data, sorting procedures are applied to reject unrealistic observations through a blacklist. The blacklist includes stations identified as unrealistic, such as for instance stations giving the same concentration for each hour of the day. Moreover, only the data representative of the horizontal resolution of the regional models (10-20 km) are selected. There is currently no uniform and reliable metadata on site representativeness available for all regions and countries of Europe. This is why we chose to

follow the work that has been done by Joly and Peuch (2012) to build an objective classification of sites, based on past validated measurements available in the Airbase database (EEA). Stations are classified between 1 and 10 depending on the characteristics of their series of measurements (diurnal cycle, "week-end effect" and high frequency variability with periods lower than 3 days). The original classification of Joly and Peuch (2012) was based on a series of data spanning from 2002 to 2009. It has been updated in MACC-II using version 7 of the Airbase database spanning from 2002 to 2011. Classes 1 to 10 cover the range from most rural background sites to most locally polluted sites. Once each station is classified we exclude those stations that have a concentration variability that is typical of locations mainly influenced by local phenomena. Only the stations with class numbers ranging from 1 to 5 for all pollutants are kept. The threshold of 5 allows us to remove the stations influenced by local phenomena while keeping a reasonable number of stations for calculating statistical indicators. This leads to a typical number in summer 2014 of : ~600 sites for ozone, ~500 sites for NO_2, ~150 sites for SO_2, ~40 sites for CO, ~400 sites for PM_{10}, ~150 sites for $PM_{2.5}$. All these data are used for the verification of the forecast products. For the verification of analyses, the developments done during MACC-II were only put into place after the end of the project. This verification is done in the following way: a list of stations not used for the assimilation is kept aside for each pollutant for verification. This list is the same every day and it has been determined so that the stations are well spread inside the domain. The ratio of observations that are kept aside for the verification of analyses is roughly 20% of the total amount of observations that are downloaded at 23UTC.

The plots of forecasts and analyses from the 7 models and the Ensemble and of their scores against observations are available daily on http://macc-raq.copernicus-atmosphere.eu/. Numerical data are publicly available and can be accessed http://www.gmes-atmosphere.eu/request_regional_data/. The full set of numerical data as listed in Table 1 is made available as soon as produced on Météo-France FTP (File Transfer Protocol) server. A subset of these data can also be interactively accessed through the Deutsches Zentrum für Luft- und Raumfahrt (DLR) World Data Center.

Major sources of uncertainties in regional AQ forecast and analyses are the quality of the emissions used, the meteorological forcings, the representation of the atmospheric physical and chemical processes, the initial and boundary conditions for the chemical species and the uncertainties in observations and assimilation methods impacting the analysis. The approach chosen in MACC-II is to use the best available emissions over Europe, high quality

meteorological forecasts and chemical boundary conditions in all seven chemistry-transport models. Therefore the variability between the forecasts of the seven models used in the ensemble comes mainly from differences in the models in the treatment of the chemical processes (homogeneous and heterogeneous, photolysis), the advection, the convective transport, the turbulent mixing and the wet and dry depositions. Other differences stem from the use of different vertical and horizontal grids. For the production of the analysis, each model uses its own assimilation system.

The inventory used for anthropogenic emissions was built primarily for modelling purposes in the frame of the MACC-II project (Kuenen et al., 2014). This is an updated version of the MACC inventory (Kuenen et al. 2011). Its resolution is 1/8° longitude x 1/16° latitude which is approximately 7 km x 7 km and it covers the UNECE-Europe for the years 2003 to 2009. The 2009 inventory is currently used in the MACC-II daily production. An important upgrade of the MACC-II inventory compared to earlier MACC inventory is the provision of a particulate matter split between Elemental Carbon, Organic Carbon, SO_4, Na and other aerosols. More details on this inventory can be found in Kuenen et al. (2014). For the biogenic sources, each model deals with its own emissions based on dynamical parameterizations and/or inventories that are detailed in the following individual model description sub-sections. Additionally, emissions from fires are taken into account using the GFASv1.1 product (Kaiser et al., 2012) available daily at 0.1°x0.1° resolution. GFASv1.1 is based on fire radiative power retrievals from data of the Moderate Resolution Imaging Spectroradiometer (MODIS) instruments aboard the Terra and Aqua satellites. The GFAS product for Day0-1 is available around 06UTC on Day0. This is soon enough to be used in the daily analysis individual production chains. At the time the individual forecasts begin for Day0, only the fire emissions from Day0-2 are available. To have less time gap between the fire emissions and the starting time of the regional forecast runs (usually around 20 UTC), an additional fire emission product available around 20:30UTC on Day0-1 using satellite observations from 15 UTC on Day0-2 to 15 UTC on Day0-1 is currently under test. In the forecasts, a persistence of the fire emissions of 3 days is assumed. This is a rounded average of the fire duration obtained by Turquety et al. (2014) from Euro-Mediterranean region from MODIS MCD64 product (Giglio et al., 2010) in the period 2003-2012.

The meteorological fields used to force the 7 CTMs are from the operational IFS (Integrated Forecasting System) daily meteorological forecasts of the European Centre for Medium-Range Weather Forecasts (ECMWF). The IFS forecast starting at 12UTC on Day0-1 is used

for the MACC-II air quality 96h forecast starting at 00UTC on Day0. For the analysis on Day0-1, the IFS forecast starting at 00UTC on Day0-1 is used.

The regional domain boundary conditions for the aerosols and gaseous species are provided by the MACC-II global assimilation and forecasting system. This forecasting system is an extension of the ECMWF meteorological IFS running at lower resolution, providing concentrations of dust, sea salt, organic matter, black carbon and sulphate aerosols (Morcrette et al. 2009, Benedetti et al. 2009) that are used to force the aerosols in the regional CTMs at the boundaries. At the end of MACC-II project (summer 2014), for the chemical species the IFS was two-way coupled to the off-line MOZART global chemical transport model (CTM). This allowed assimilation of satellite data for O_3, NO_2, and CO in the IFS itself, while the detailed chemical processes were handled in the MOZART model (Flemming et al. 2009, Stein et al. 2012, Inness et al. 2013). Since 18 September 2014, the MACC-II global assimilation and forecasting system has been upgraded to a fully integrated system for aerosols and chemical species. Instead of the coupling with the MOZART model, the chemistry is now treated on-line in the IFS using chemistry modules based on the TM5 model (Huijnen et al., 2010). This new system is named Composition-IFS (C-IFS) and is further described in Flemming et al. (2014). The chemical mechanism in the TM5 operational version of C-IFS is based on a modified version of the Carbon Bond 5 (CB05) scheme (Williams et al., 2013, Yarwood et al., 2005).

Based on all the inputs described above, each of the centres in charge of the 7 models runs its production locally and transfers its forecast and analysis files to Météo-France (referred to central production centre hereafter). The general organisation of the MACC-II air quality forecasts and analysis system is summarized in Fig. 1. Tables 3 and 4 give the general features of the seven individual models and of their analysis system. A short description of the seven individual models and of the ensemble is given in the following sections. More details can be found in the MACC-II 6-monthly reports (http://www.gmes-atmosphere.eu/documents/maccii/deliverables/ens/).

2.2 CHIMERE forecast and analysis system

CHIMERE is an Eulerian chemistry-transport model able to simulate concentrations fields of gaseous and aerosols species at a regional scale (Menut et al., 2013a). The model is developed under the GPL licence (http://www.lmd.polytechnique.fr/chimere/). CHIMERE is used for

analysis of pollution events, process studies, (Bessagnet et al., 2009; Beekmann and Vautard, 2010), experimental and operational forecast (Rouil et al., 2009), regional climate studies and trends, (Colette et al., 2011), among others.

CHIMERE calculates and provides the atmospheric concentrations of tens of gas-phase and aerosol species over local (e.g. urban) to continental domains (from 1 km to 1 degree resolution). Vertically, the model is able to simulate the whole troposphere. The gaseous species are calculated using the MELCHIOR2 scheme and the aerosols using the scheme developed by Bessagnet et al. (2004). This module takes into account species such as sulphate, nitrate, ammonium, primary organic matter (POM) and elemental carbon (EC), secondary organic aerosols, sea salt, dust and water. These aerosols are represented using 8 bins, from 40 nm to 40 um, in diameter. The life cycle of the aerosols is completely represented with nucleation of sulphuric acid, coagulation, adsorption/desorption, wet and dry deposition and scavenging. This scavenging is both represented by coagulation with cloud droplets and precipitation. The formation of SOA is also taken into account (Bessagnet et al., 2009).

Biogenic emissions are calculated using the MEGAN emissions scheme (Guenther et al., 2006) which provides fluxes of isoprene and monoterpenes. The mineral dust emissions are calculated using the (Alfaro and Gomes, 2001) scheme, forced by satellite soil and surface data (Menut et al., 2013b).

The CHIMERE assimilation system for operational products is based upon hourly optimal interpolation processing of surface observations for O_3 and PM_{10} (Honoré et al, 2008). During MACC-II, an Ensemble Kalman filter has been also developed for ozone analysis (Gaubert et al., 2014).

CHIMERE is fully dedicated to regional air pollution modelling. It includes a comprehensive representation of the aerosol with secondary organic (SOA) and inorganic aerosols (SIA). CHIMERE has a chemical scheme specifically designed to reproduce the photochemical activity in the lower part of the troposphere (for air quality purposes). In terms of point that may need to be improved, the vertical resolution is composed of 8 levels up to 500 hPa, meaning that the models need to be fed with realistic top conditions. The assimilation is so far limited to O_3 and PM_{10} and for the surface layer.

2.3 EMEP forecast and analysis system

The EMEP/MSC-W model (hereafter referred to as 'EMEP model') has been developed at the EMEP Meteorological Synthesizing Centre-West at the Norwegian Meteorological Institute. The model has been publicly available as open source code since 2008, and a detailed description is given in Simpson et al. (2012).

The numerical solution of advection is based on Bott (1989). The turbulent diffusion coefficients are calculated for the whole 3D model domain on the basis of local Richardson number, and the planetary boundary layer (PBL) height is calculated using methods described in Simpson et al. (2003). Dry deposition uses a resistance analogy combined with stomatal and non-stomatal conductance algorithms (Simpson et al., 2003; Tuovinen et al., 2004), whereas wet deposition uses scavenging coefficients applied to the 3-D rainfall, including both in-cloud and sub-cloud scavenging of gases and particles. The chemical scheme couples the sulphur and nitrogen chemistry to the photochemistry using about 140 reactions between 70 species (Andersson-Sköld and Simpson, 1999; Simpson et al. 2012).

The methodology for biogenic emissions builds on maps of 115 forest species generated by Köble and Seufert (2001). Emission factors for each forest species and for other land classes are based on Simpson et al. (1999), updated with recent literature (see Simpson et al. (2012) and references therein), and driven by hourly temperature and light using algorithms from Guenther et al. (1995). Other natural emissions include marine emissions of dimethyl sulphide, and SO_2 from volcanoes.

The standard model version distinguishes two size fractions for aerosols, fine aerosol ($PM_{2.5}$) and coarse aerosol (PM_{10} excluding $PM_{2.5}$). The aerosol components presently accounted for are sulphate, nitrate, ammonium, anthropogenic primary particulate matter, sea salt and desert dust. Also aerosol water is calculated. The parameterisation of dry deposition for aerosols follows standard resistance formulations, accounting for diffusion, impaction, interception, and sedimentation. Wet scavenging is treated with simple scavenging ratios, taking into account in-cloud and sub-cloud processes. For secondary organic aerosol (SOA) the so-called 'EmChem09soa' scheme is used, which is a slightly simplified version of the mechanism described by Bergström et al. (2012).

The EMEP data assimilation system (EMEP-DAS) is based on the 3D-Var implementation for the MATCH model (Kahnert, 2008, 2009). The background error covariance matrix is estimated following the NMC method (Parrish and Derber, 1992). Currently, the EMEP-DAS delivers analyses for NO_2, using NO_2 columns of OMI and in situ measurements of NO_2 surface concentrations. The assimilation window is 6 hours, 4 times per day.

The EMEP model performs well especially for particulate matter, as it includes carefully evaluated representations of both primary and secondary organic aerosols, in addition to inorganic aerosols, elemental carbon, sea salt, mineral dust and water. Another strength is that its domain extends throughout the whole troposphere, thus taking accurate account of long-range transport of pollutants in the free troposphere. As the EMEP model is designed mainly for background concentrations, urban increments have not been implemented as in some other models with equally coarse resolution, leading to somewhat lower performance in urban and sub-urban areas. However, being one of the main research tools under the UN LRTAP convention, the EMEP model is evaluated continuously against measurements of a large range of chemical parameters (including air concentrations, depositions, and trends) ensuring modelling capability with very good overall performance (e.g. Jonson et al., 2006; Fagerli and Aas, 2008; Genberg et al., 2013). A weakness of the analysis chain until the end of 2014 was that only NO_2 was assimilated. However, since early 2015 ozone has been assimilated.

2.4 EURAD-IM forecast and analysis system

EURAD-IM is an Eulerian meso-scale chemistry transport model involving advection, diffusion, chemical transformation, wet and dry deposition and sedimentation of tropospheric trace gases and aerosols (Hass et al., 1995, Memmesheimer et al., 2004). It includes 3d-var and 4d-var chemical data assimilation (Elbern et al., 2007) and is able to run in nesting mode. EURAD-IM has been applied on several recent air pollution studies (Monteiro et al., 2013; Zyryanov et al., 2012; Monteiro et al, 2012; Elbern et al., 2011; Kanakidou et al., 2011).

The positive definite advection scheme of Bott (1989) is used to solve the advective transport. An Eddy diffusion approach is used to parameterize the vertical sub-grid-scale turbulent transport. The calculation of vertical Eddy diffusion coefficients is based on the specific turbulent structure in the individual regimes of the planetary boundary layer (PBL) according to the PBL height and the Monin-Obukhov length (Holtslag and Nieuwstadt, 1986). A semi-implicit (Crank-Nicholson) scheme is used to solve the diffusion equation.

Gas phase chemistry is represented by the Regional Atmospheric Chemistry Mechanism (RACM) (Stockwell et al., 1997) and an extension based on the Mainz Isoprene Mechanism (MIM) (Geiger et al., 2003). A two-step Rosenbrock method is used to solve the set of stiff ordinary differentials equations (Sandu et al., 2003; Sandu and Sander, 2006). Photolysis frequencies are derived using the FTUV model according to Tie et al. (2003). The radiative

transfer model therein is based on the Tropospheric Ultraviolet-Visible Model (TUV) developed by Madronich and Weller (1990). The modal aerosol dynamics model MADE (Ackermann et al., 1998) is used to provide information on the aerosol size distribution and chemical composition. To solve for the concentrations of the secondary inorganic aerosol components, a FEOM (fully equivalent operational model) version, using the HDMR (high dimensional model representation) technique (Rabitz et al., 1999; Nieradzik, 2005), of an accurate mole fraction based thermodynamic model (Friese and Ebel, 2010) is used. The updated SORGAM module (Li et al., 2013) simulates secondary organic aerosol formation. Biogenic emissions are calculated in the EURAD-IM CTM with the Model of Emissions of Gases and Aerosols from Nature (MEGAN) (Guenther et al., 2012).

The gas phase dry deposition modelling follows the method proposed by Zhang et al. (2003). Dry deposition of aerosol species is treated size dependent using the resistance model of Petroff and Zhang (2010). Wet deposition of gases and aerosols is derived from the cloud model in the EPA Models-3 Community Multiscale Air Quality (CMAQ) modelling system (Roselle and Binkowski, 1999).

The EURAD-IM assimilation system includes (i) the EURAD-IM CTM and its adjoint, (ii) the formulation of both background error covariance matrices for the initial states and the emission factors, (iii) the observational basis and its related error covariance matrix, and, (iv) the minimisation including the transformation for preconditioning. The quasi-Newton limited memory L-BFGS algorithm described in Nocedal (1980) and Liu and Nocedal (1989) is applied for the minimization. Following Weaver and Courtier (2001) with the promise of a high flexibility in designing anisotropic and heterogeneous influence radii, a diffusion approach for providing the background error covariance matrices is implemented.

One of the EURAD-IM strength is that it includes a comprehensive treatment of aerosol dynamics and chemistry. Parameterisations of the formation of secondary particles are temperature dependent for both the inorganic and organic components. However, the complexity of the aerosol components of EURAD-IM is as yet not supported by sufficiently known emission rates of particle types, as well as for organic gaseous precursor compounds, especially from biogenic sources. Another strength of the EURAD-IM system is its ability to assimilate chemical data from a wide range of instruments ranging from surface or airborne *in situ* data to retrievals from several satellites, which are then defining the initial values.

2.5 LOTOS-EUROS forecast and analysis system

The 3D chemistry-transport model LOTOS-EUROS (Schaap et al., 2008) is developed by the Dutch institutes TNO (www.tno.nl), RIVM (www.rivm.nl) and, more recently, KNMI (www.knmi.nl). It is used for regional-scale air-quality forecasts in Europe and the Netherlands (de Ruyter de Wildt et al., 2011). The LOTOS-EUROS model has participated in several international model intercomparison studies addressing ozone (Van Loon et al., 2007; Solazzo et al., 2012a) and particulate matter (Cuvelier et al., 2007; Vautard et al., 2007; Stern et al., 2008; Solazzo et al., 2012b). These studies have shown that the model has a performance comparable to other European regional models. In the past three year, three major updates of the LOTOS-EUROS model have been implemented, moving from version 1.7 to version 1.10. Detailed update information can be found on the model web page, http://www.lotos-euros.nl. Since the end of MACC-II, the latest update to v1.10 implemented operationally consists of changes in the SO_2 to SO_4 conversion rate, use of AQMEII conventions for the fine/coarse dust assignment, update of resistances for e.g. ozone (leading to an overall ozone increase), and improvement of the treatment of fire emissions.

The model extends up to 3.5 km above sea level, with three dynamic layers and a fixed 25m thick surface layer. The lowest dynamic layer is the mixing layer, followed by two reservoir layers. The height of the mixing layer is obtained from the ECMWF meteorological input data used to drive the model. Transport is based on the monotonic advection scheme developed by Walcek (2000). Gas phase chemistry is described using the TNO CBM-IV scheme (Schaap et al., 2008). Hydrolysis of N_2O_5 is described following Schaap et al. (2004). Aerosol chemistry is represented using ISORROPIA-2 (Fountoukis and Nenes, 2007). The aerodynamic resistance is calculated for all land use types separately. Below cloud scavenging is described using simple scavenging coefficients for gases (Schaap et al., 2004) and particles (Simpson et al., 2003). Dry deposition is based on the well-known resistance approach, with the DEPAC parameterization for gases (Wichink Kruit et al., 2012) and the Zhang et al. (2001) parameterization for particles.

Biogenic isoprene emissions are calculated following the mathematical description of the temperature and light dependence of the isoprene emissions, proposed by Guenther et al. (1993), using the actual meteorological data. For land use the CORINE/Smiatek database has been enhanced using the tree species map for Europe made by Koeble and Seufert (2001). Total PM10 in the LOTOS-EUROS model is composed of chemically unspecified primarily

PM in the fine and coarse mode, black carbon, dust, ammonium, sulphate, nitrate and sea salt (Na in the fine and coarse mode).

The LOTOS-EUROS model is equipped with a data assimilation package with the ensemble Kalman filter technique (Barbu et al., 2008; Timmermans et al., 2009; Curier et al., 2012). Data assimilation for the MACC-II daily analyses is performed with surface ozone observations (Curier et al., 2012). An extension to other surface and satellite data is foreseen in the near future.

The LOTOS-EUROS model has been designed as a model of intermediate complexity, to favor short computation times. For this, the vertical top of the operational model version is limited and covers only the boundary layer and reservoir layers (up to 3.5 km); effectively, the model therefore employs 4 dynamic layers only. Concentrations from the free-troposphere are taken from the global boundary conditions, and therefore fully incorporate the knowledge, assimilations, and validation efforts present in the global model. A major weakness is that secondary organic aerosols are currently not included; instead, a bias correction for total PM is used to account for the missing aerosols. In spite of the limited complexity, the model performs well in simulation of O_3 (Curier et al., 2012) and has a skill to forecast the observed variability in PM_{10} (de Ruyter de Wildt et al., 2011). Apart from the relative short run-through time, the strength of the model is in the detailed description of anthropogenic emissions, since close cooperation with the developers of the TNO-MACC emission inventory; this is for example shown by excellent simulation of boundary layer NO_2 (Vlemmix et al., 2015).

2.6 MATCH forecast and analysis system

The MATCH model (Multi-scale Atmospheric Transport and Chemistry model) has been developed at SMHI over the past 20 years and is applied for emergency purposes as well as for regional scale chemistry modelling (Langner et al., 1998; Robertson et al., 1999).

The transport is described by a Bott-like mass conservative scheme (Bott, 1989; Robertson et al., 1999). For the vertical diffusion an implicit mass conservative scheme is used where the turbulent exchange coefficients for neutral and stable conditions are parameterized following Holtslag and Moeng (1991). In the convective case the turbulent Courant number is directly determined from the turn-over time in the atmospheric boundary layer.

548 The dynamical core of the model contains initialization and adjustment of the horizontal wind
549 components based on a procedure proposed by Heimann and Keeling (1989). This is
550 important to ensure mass conservative transport for interpolated input weather data,
551 specifically for the transport scheme used.

552 Boundary layer parameterization is determined from surface heat and water vapour fluxes as
553 described by van Ulden and Holtslag (1985) for land surfaces, and Burridge and Gadd (1977)
554 for sea surfaces. The boundary layer height is calculated from formulations proposed by
555 Zilitinkevich and Moronov (1996) for the neutral and stable case and from Holtslag et al.
556 (1995) for the convective case. These parameterizations drive the formulations for vertical
557 diffusion and dry deposition where for the latter a resistance approach is used (Andersson et
558 al. 2007). In-cloud and sub-cloud wet deposition is implemented following Andersson et al.
559 (2007). The photochemistry scheme is to large extent based on the EMEP chemistry scheme
560 (Simpson et al., 1993), with some updates where a modified production scheme for isoprene
561 is the most notable based on the so-called Carter-1 mechanism (Carter, 1996; Langner et al.,
562 1998).

563 Aerosols are described for 4 bins and only for secondary inorganic aerosols, dust and primary
564 organic compounds at the moment. Inclusion of SOA is under testing. Sea salt emissions are
565 dynamically described following Foltescu et al. (2005). A module for wind driven dust
566 emissions is under testing that follows Schaap et al. (2005).

567 A 3D variational data assimilation scheme is used with spectral transformation (Kahnert,
568 2008). The limitation then is that background covariance structures are described as isotropic
569 and homogeneous, however not necessarily the same for different wavenumbers, and derived
570 from the so-called NMC-method (Parish and Derber, 1992). The advantage though is that the
571 background error matrix becomes block diagonal and there are no scale separations as the
572 covariance between spectral components are explicitly handled. The block diagonal elements
573 are the covariance between wave components at different model layers and chemical
574 compounds.

575 The strength of the MATCH model is that it spans vertically the troposphere and makes use of
576 the same vertical layers as provided from the IFS model up to 300 hPa. This means about 50
577 layers in the vertical and the lowest one just 20 m thick and about 15 in the boundary layer.
578 Using the same vertical resolution as the IFS model is an advantage because no vertical
579 interpolation is required. Nevertheless, since the MATCH model has been developed mainly
580 using HIRLAM data with a coarser vertical resolution, the use of the high resolution vertical

levels from IFS may lead to less accurate chemistry forecasts compared to HIRLAM version. A weakness is missing SOA and wind-blown dust in the PM description.

2.7 MOCAGE forecast and analysis system

The MOCAGE (Model Of atmospheric Chemistry At larGE scale) model (Josse et al. 2004, Dufour et al. 2004) has been developed at Météo-France since 2000. Its assimilation system has been developed jointly with CERFACS. This model and its assimilation system have been successfully used for tropospheric and stratospheric research (e.g. Bousserez et al. 2007; Barré et al. 2013, 2014; Lacressonnière et al. 2014) and also for operational purposes (Rouïl et al. 2009).

MOCAGE uses the semi-lagrangian advection scheme from Williamson and Rasch (1989) for the grid-scale transport, the parameterization of convective transport from Bechtold et al. (2001) and the turbulent diffusion parameterization from Louis (1979). Dry deposition is based on the approach proposed by Wesely (1989). The wet deposition by the convective and stratiform precipitations follows Mari et al. (2000) and Giorgi and Chameides (1986). MOCAGE includes the RACM scheme for tropospheric chemistry (Stockwell et al., 1997) and the REPROBUS scheme for stratospheric chemistry (Lefèvre et al., 1994). Biogenic emissions in MOCAGE are fixed monthly biogenic emission from Guenther et al. (1995).

The aerosol module of MOCAGE follows a bin approach and includes so far the primary aerosols: dust (Martet et al. 2009), sea salts, black carbon (Nho-Kim et al. 2005) and organic carbon. Recent updates of the primary aerosol module and corresponding evaluation can be found in Sič et al. (2014).

MACC-II operations use a variational assimilation system based upon MOCAGE and the PALM coupler, which has been developed during the ASSET European project (Geer et al., 2006; Lahoz et al., 2007). The system, recently renamed VALENTINA, has been used to compute global and regional re-analyses of atmospheric composition in multiple studies (El Amraoui et al., 2008; Massart et al., 2009; Barré et al. 2013, 2014; Emili et al., 2014). The assimilation algorithm employed for MACC-II analyses is a 3D-Var with assimilation windows of one hour length (Jaumouillé et al., 2012), corresponding to the frequency of surface measurements. The assimilation has first been set for surface ozone analyses and in MACC-III it has been extended to surface NO_2. The specification of the background and observation errors is done based on the evaluation of historical time-series of observations and

model values. The horizontal error correlation has a Gaussian shape and its typical length is set to 0.4 degrees for ozone and 0.1 degrees for NO_2, to account for the larger variability of NO_2 at fine spatial scales. The vertical error correlation length is set to 1 model grid point for all species (~100 m). As a consequence, assimilation increments linked to surface observations are confined in the planetary boundary layer.

The strength of MOCAGE is that it simulates the air composition of the whole troposphere and lower stratosphere. Thus it provides a full representation of transport processes, in particular boundary layer-troposphere and troposphere-stratosphere exchanges, and the time evolution of stratospheric conditions for accurate photolysis rate calculations at the surface. The MOCAGE assimilation system in its MACC configuration produces robust analyses for both O_3 and NO_2 as illustrated in the annual reanalysis reports (http://www.gmes-atmosphere.eu/documents/maccii/deliverables/eva/). At the end of the MACC-II project, the main weakness of MOCAGE was the lack of secondary aerosols. Inorganic secondary aerosols have been developed recently and will be included in the next MACC operational version (Guth et al., 2015). This new feature is also used in the current development of PM_{10} assimilation.

2.8 SILAM forecast and analysis system

SILAM is a meso-to-global scale dispersion model (Sofiev et al, 2008), see also the review Kukkonen et al., (2012), http://silam.fmi.fi) that is used for atmospheric composition, emergency, composition-climate interactions, and air quality modelling purposes. The model has been applied with resolutions ranging from 1km up to 3 degrees, incorporates 8 chemical and physical transformation modules and covers the troposphere and the stratosphere. The model is publicly available since 2007 and is used as operational and research tool.

The model has two dynamic cores: Lagrangian (Sofiev et al., 2006), primarily used in emergency-type applications, and Eulerian (Galperin, 2000; Sofiev, 2002) used in atmospheric composition, climate, and air quality-related applications, including MACC-II. The MACC-II operational SILAM v.5.2 uses the simple dry deposition scheme of (Sofiev, 2000) for gases and a new approach for aerosols (Kouznetsov and Sofiev, 2012), which covers particle sizes from 1 nm up to ~ 50 μm of effective aerodynamic size. The wet deposition scheme used in MACC-II simulations calculates the 3-D removal coefficient and distinguishes between sub- and in-cloud scavenging, large-scale and convective

precipitations, as well as between rain and snow (Sofiev et al., 2006). Boundary layer parameterization follows (Sofiev et al., 2010), whereas in the free troposphere and the stratosphere turbulence is computed following IFS approach and corresponding turbulent length scale.

Two chemical schemes are used: the CBM-4 gas-phase chemistry mechanism and own development for heterogeneous chemical transformations and inorganic aerosol formation after (Sofiev, 2000). Aerosols in SILAM are represented via sectional approach with species-specific size spectra. The aerosol species include primary anthropogenic aerosols, divided into $PM_{2.5}$ and PM_{10}, secondary inorganic aerosols (sulphates, nitrates and ammonia), and sea salt aerosols.

The forecasts utilise the BVOC emission term based on NatAir project results (Poupkou et al., 2010) and own development for the sea-salt emission (Sofiev et al., 2011).

The data assimilation system of SILAM consists of 3D-VAR and 4D-VAR modules (Vira and Sofiev, 2012). The MACC-II near-real time analysis suite uses the 3D-VAR method and assimilates hourly surface observations of NO_2, O_3 and SO_2. PM observations have been assimilated in reanalysis simulations (Vira and Sofiev, 2015). The 4D-VAR methodology is utilised in re-analysis mode for pollen.

The model evolution from the MACC-II v.5.2 towards v.5.4 that will become operational in early-2015, include several important updates. The dry deposition scheme will follow the resistance analogy with extensions after (Simpson et al., 2003). Wind-blown dust will be included via lateral boundary conditions in the next release of operational SILAM v.5.4, together with a secondary organic aerosol module and fire emission.

A strong point of SILAM is the extensive treatment of secondary inorganic aerosol formation, which is reproduced quite well, according to several evaluation exercises and model inter-comparisons. Together with the detailed deposition scheme, this leads to good scores for $PM_{2.5}$, especially in winter when inorganic aerosols are dominant. The current limitation of the model is the secondary organic aerosols formation that makes use of the volatility-based model but it is not yet incorporated in the operational simulations, being tested in research projects. A workaround of this limitation is included in the data assimilation modules, which allow assimilation of both in-situ and remote-sensing measurements of gaseous and particulate species. The module now allows for the PM and AOD observations being

assimilated into an unspecified particulate matter, which is then treated as inert aerosol, thus compensating for the lack of secondary organic particles.

2.9 ENSEMBLE forecast and analysis system

To process the ensemble, all seven individual models are first interpolated to a common 0.1°x0.1° horizontal grid. For each grid point, the ensemble model (referred as the ENSEMBLE hereafter) value is calculated as the median value of the individual model forecasts or analyses available. The median is defined as the value having 50% of individual models with higher values and 50% with lower values. This method is rather insensitive to outliers in the forecasts or analyses and is very efficient computationally. These properties are useful from an operational point of view. The method is also little sensitive if a particular model forecast or analyses is occasionally missing. The performances of the ensemble median are discussed in section 3. For the forecasts, the ensemble is produced for all levels and all species (core and additional). For the analyses, the individual assimilation systems provide only analyses at the surface level and do not produce analyses for all species yet. At the end of MACC-II, ozone was the only species that was produced by 6 of the models. For other species, analyses from less than 5 models were available. This is why the ensemble analysis in MACC-II was only calculated for ozone. It has been extended to NO_2 in 2015 since more models will produce NO_2 analyses.

3. Evaluation of the performances of the system

3.1 General description

The evaluation of the performances of a forecast system is a necessary step rating its quality and thus proving its usefulness. The MACC-II air quality forecasts are evaluated against the NRT AQ surface monitoring data detailed in section 2.1. Note that this set of data is fully independent of the forecast since the analyses assimilating the NRT AQ data are produced too late to be used to initialise the forecasts. The tools to assess the performances of the analyses are not yet in place but this is planned to be ready in 2015. Since the focus of the MACC-II regional system over Europe is on air quality, meaning air composition close to the surface, no column observations (ground based or from satellite) or upper air *in situ* measurements (i.e. on board aircraft) are used operationally to evaluate the system performances.

The forecast performances are measured using the five statistical indicators detailed in the Appendix: the mean bias (MB), the root mean square error (RMSE), the modified normalized mean bias (MNMB), the fractional gross error (FGE) and the correlation. These statistical measures, when taken together, provide a valuable indication of the model performances. Taylor diagrams are also used to combine root mean square errors and correlations.

The performances of the MACC-II regional AQ forecasts are assessed operationally by several means:

- on a daily basis with plots of statistical indicators and charts available on the MACC-II regional website (http://macc-raq.gmes-atmosphere.eu/),
- on a 6 monthly basis in reports including plots of statistical indicators over two periods of 3 months (winter+spring or summer+autumn) and analysis of these indicators (http://www.gmes-atmosphere.eu/documents/maccii/deliverables/ens/).

Additionally, on a 6 monthly basis, reports are especially dedicated to the scientific analysis of the forecasts of the 7 models and of the ensemble in the Mediterranean area (http://www.gmes-atmosphere.eu/documents/maccii/deliverables/ens/). The Mediterranean area is recognized as challenging for models, in particular under summer conditions with very active photochemistry and because of its large variety of emission sources.

The performances of the NRT analysis are not presented in this paper since there is only an ensemble production of one species (ozone) and the daily verification procedure against an independent dataset was not yet in place at the end of MACC-II project.

3.2 Availability statistics

The MACC-II regional air quality forecasting and analysis system is currently under a pre-operational status that can be seen as the demonstrator of a future operational system. Correct working of 7 model chains and of the Ensemble chain is monitored on working hours only since, at this stage, there was no funding yet for a 7day/7day 24h/24h control. Nevertheless, in its pre-operational configuration the production chains are reliable with availability in time (see Table 2) of the 7 individual forecasts and analysis generally above 85% during MACC-II. During the past year, the production suffered from failures because of the many changes that were applied to the individual and central systems to fit with fully operational standards (data format, file transfer, databases, processing softwares, …). The operationalisation being nearly fully settled, the reliability has been improved since the end of MACC-II (generally above

90%). The Ensemble forecast and analysis productions have been available 100% of the time since September 2012. This high performance was achieved because the ENSEMBLE can be produced even if all the 7 models are not available.

3.3 Example of the forecast of two ozone episodes between the 10th and the 13th of June 2014

In this section, we illustrate the performances of the MACC-II AQ forecasts for a case study of ozone pollution events that took place between the 10th and the 13th June 2014. A more in-depth analysis of the individual model and of the ENSEMBLE performances is done over longer time periods in Section 3.4.

During the case study period, there were two regional areas with high ozone concentrations (> 120 mg m^{-3}) occurring at the same time, one over Austria and surrounding regions (South of Germany and Hungary), and one over the South East of France and the North of Italy. This is illustrated by Fig. 2 displaying the maps of the 15h forecasts for the 10th of June at 15UTC of ozone at surface from the ENSEMBLE together with the available observations. Note that unfortunately no observation in Italy was available during the time period considered. Even if the comparison is limited by the missing observations, Fig. 2 shows that the ensemble median captures the two ozone episodes.

For illustration of the system performance, the surface station measurements are compared in Fig. 3 to the forecast. We plot the model forecasts using EPSgrams that give a graphical representation of the spread of the 7 models and therefore an estimate of the uncertainty over the 4 days of the forecast. Operationally, EPSgrams are built daily for 40 major cities in Europe and made available on the MACC regional web site. Here EPSgrams are calculated and plotted for the same locations as the measurements (Fig. 3) from the forecast started on the 10th of June at 00UTC. Note that, in Fig. 3, EPSgrams are 3-hourly while observations are 1-hourly. In the observations (left panel), the "Austrian" episode is highest on the 10th of June in Fechenheim (Germany) and on the 11th of June in Hallein (Austria) and Sopron (Hungary) with values reaching 200 µg m^{-3} at Sopron. The "French" episode peaks at 250 µg m^{-3} at Sausset (France) with daily maxima over 150 µg m^{-3} from the 10th to the 13th of June for all three stations.

For the ozone peak event around Austria, there is generally a good consistency of the day-to-day trend provided by the seven models compared to the AQ station observations. For Sopron

771 station there is a main peak in the model on the 11th of June as in the observations. For
772 Fechenheim, the forecast gives highest concentrations on the 10th of June as measured, and
773 also reproduces the anomaly recorded in the observations in the morning of the 11th of June.
774 For this "Austrian" ozone episode, the spread between the 7 models is very reasonable
775 (generally less than 30 μg m^{-3} for the 25%-75% range), showing the good consistency
776 between the models with slightly more spread between the forecasts for the highest peak
777 times. There is an exception in Fechenheim on the 10th of June where the 7 models exhibit a
778 large spread. This can be explained by the effect of complex topography combined with
779 specific meteorological conditions that lead to different behaviours of the models which have
780 different horizontal grids and orography.

781 Even if the day-to-day trend is well reproduced by the models, ozone median values are often
782 lower during daytime peaks than the observations by 30 to 50 μg m^{-3} but the maxima of the 7
783 models are nevertheless close to those observed. There are also cases when the ensemble
784 median forecasts higher peaks than measured as in Fechenheim on the 10th of June. This can
785 also be seen in the map in Fig. 2 where some observations are lower than the ensemble
786 median. During nighttime, the ozone median is close to the observed values.

787 For the ozone event in the south of France, the comparison shows also a good consistency
788 between the diurnal variations of the models compared to observations. Most of the 7 models
789 are over 120 μg m^{-3} for each of the 4 days forecasted. Nevertheless, at Sausset the very high
790 ozone peak measured on the 10th of June (over 240 μg m^{-3}) is underestimated in all 7
791 forecasts. The very small spread of the models indicates a possible error in the meteorological
792 forecast for this day and/or in the emissions. Sausset is located on the Mediterranean coast,
793 west to Marseille industrial city. On this particular day IFS forecasts an eastern wind with
794 high NOx from Marseille limiting the daytime production of ozone by the models compared
795 to observations. For Plan d'Aups, there is a very large spread of the models, particularly on
796 the 10th of June. This can be explained by the effect of sea and land breezes on this date
797 combined with steep orography and the presence in the vicinity of a pollution plume with
798 NOx titrated ozone that leads to model differences. In this case (Plan d'Aups), models do not
799 reproduce observations. While for the other stations, the behaviour of the ensemble is good.
800 For St Rémi, the models perform well with a small spread and diurnal variations close to the
801 measurements. In particular, the increase of the night minimum concentration from day to day
802 is well forecasted. Similarly to the Austrian area, the ozone median concentrations are more
803 often lower than observed, but not always, as shown at Sausset on the 13th of June and St

804 Rémi on the 10th of June. In the case of underestimation of the ensemble median, the
805 maximum of the individual models is generally close to those measured at the French stations.
806 Note that for both the "Austrian" and "French" ozone episodes, there is no significant
807 degradation of the forecast skills at Day3 and Day4 indicating that uncertainty in ozone
808 forecasts is more driven by inherent uncertainty in chemistry transport models and part of its
809 input than by uncertainty of meteorological forecast.

810 For further evaluation, Fig. 4 displays the MB, MNMB, RMSE, FGE and R (defined in
811 Appendix) of ozone of the seven individual models and the ENSEMBLE calculated using the
812 representative observations available over the whole European domain. These statistics are
813 based on seven consecutive 96h forecasts run every day from the 9th of June to the 15th of
814 June. This figure shows that there is a spread of the 7 models and that the ENSEMBLE
815 generally gives the best scores with MNMB between 0.2 and -0.1, FGE between 0.15 and 0.4
816 and correlations up to 0.75 during daytime. All the models, including the ENSEMBLE,
817 exhibit a diurnal cycle with higher correlations and lower RMSE and FGE during daytime
818 (when ozone is high) than during nighttime. Five of the models have a positive MB on
819 average and the other two a negative MB on average. The statistics are only calculated here
820 on one week but there is a good consistency with scores based on longer time series, as shown
821 and analysed in detail in Section 3.4.

822 To illustrate the behaviour of the MACC-II ensemble system in the case when some of the 7
823 models are missing for the production of the ENSEMBLE, we selected as an example the
824 period of the 9th to the 15th of June 2014 corresponding to the ozone episodes discussed in
825 Section 3.2 and we compared the following ensembles:

826 - 'MEDIAN 7', the operational ensemble method which is the median of the 7 models
827 (=ENSEMBLE) as presented in Fig. 4,

828 - 'MEDIAN 5', built on 5 individual models, after filtering out the best and the worst models,
829 according to the criterion described below,

830 - 'MEDIAN 3', built on 3 individual models, after filtering out the two best and the two worst
831 models, according to the criterion described below,

832 - '1BEST', the best model.

833 By removing at the same time the best (or two best) and the worst (or two worst) models we
834 estimate an "average situation". Since the relative performances of individual models vary in
835 time and space, the criterion to order the 7 individual models from worst to best is measured

by their RMSE over the 7 days of the verification between 12 UTC and 18 UTC (ozone peak time). This criterion is chosen on the basis that we look for the model best reproducing the high daytime ozone levels. RMSE is seen as the most objective criterion since MB and NMNB can include compensating effects and since there is a low spread between the models in the FGE. From this, the best model is displayed in purple colour in Fig. 4c and the worst in brown colour.

Results of the sensitivity experiments are shown in Fig. 5. This figure confirms that the ensemble median (MEDIAN 7) using all 7 models performs generally better than the best model on all statistical indicators. When only five models (excluding the best and the worst) are available to calculate the ensemble, all scores show only very slight differences with the ENSEMBLE (MEDIAN 7) based on 7 models. Going to only three models to calculate the ensemble (MEDIAN 3) leads to statistical indicators degraded compared to the ensemble from 7 (MEDIAN 7) or 5 (MEDIAN 5) models but performs generally better than the best model (1BEST). This indicates that using an ensemble of models, even if reduced, is more useful than using a single model event of very good quality. This also shows that with 5 models available (that may happen in case of problems of production of 2 of the 7 models), the ensemble is still robust compared to observations.

In our tests we disregarded the worst (or 2 worst) and best (or two best) models on a RMSE criterion but Kioutsioukis and Galmarini (2014) showed that there is an impact of the quality of the models chosen on AQ ensemble performances. To go a step further, a more comprehensive study is done in Section 3.4 over a longer time period.

3.4 Statistical performances of the forecasts on a seasonal basis

Additionally to the production of daily skill scores, statistical indicators are calculated for ozone, NO_2 and PM_{10} at surface on a seasonal basis since September 2009 for each of the seven models and for the ENSEMBLE. These skill scores and the analysis of their seasonal and year-to-year evolutions are presented in 6 monthly reports, each including 2 seasons. The model statistical indicators are calculated against measurements from the European AQ surface station network available in NRT and selected as detailed in Section 2.1. So far, the data provision in NRT is not fully operational. Therefore, there is some variability with time of the number of data available and of their location. Also, the spatial coverage of the surface AQ network in Europe is very inhomogeneous with a high density of stations in France,

Germany, UK, Belgium and The Netherlands. Thus the statistical indicators are more representative of the system skills for these countries.

Here we only focus on the performances of the system for the last year of MACC-II to document its status at the end of the project. We only analyse the two main pollutants for the season during which exceedances of regulatory levels are more likely to be encountered: ozone in summer (1st of June to 1st of September 2014) and PM_{10} in winter (1st of December 2013 to 1st of March 2014). We are not showing scores for previous years since the use of a different set of surface observations from one year to another does not allow a fair comparison of the model skills.

MB, MNMB, RMSE, FGE and R for ozone in summer 2014 from the 7 models and the ENSEMBLE are shown in Fig. 6. One main feature, that is common to all models including the ENSEMBLE, is that there is no day-to-day degradation of MB, MNMB, and FGE indicators from Day0 to Day3 and a slight increase of the RMSE around 15UTC (about 1 μg m^{-3}). This indicates that the values of the surface ozone concentrations are not affected on average by the day-to-day degradation of the meteorology but are rather driven by other processes such as emissions of precursors and chemistry. However, correlations (Fig. 6e) tend to decrease from Day0 to Day3. This tendency was also found in scores calculated for previous years. Correlations give a measure of the ability of each model to fit the time variations of ozone regardless of concentration biases. Therefore, correlations are more sensitive to the meteorological forecast skills than MB, MNMB, RMSE and FGE. Nevertheless, the decrease of the correlation with forecast day is slow.

In Fig. 6 there is a marked diurnal cycle of all statistical indicators for all models which leads to a similar diurnal cycle in the ENSEMBLE scores. MNMB, FGE and R show best performances peaking at 15UTC and worst peaking at 06UTC for each of the 4 days of the forecast. This means that all models are able to simulate the ozone daytime photochemistry with the given setup of MACC-II (IFS forecasts for meteorology, C-IFS for chemical boundary conditions and GFAS and TNO emissions). For all models, the diurnal cycle in the statistical indicators can be at least partly explained by uncertainties in the diurnal cycle of the emissions of ozone precursors used in the individual models. This is illustrated by CHIMERE correlation at night which is better than most of the other models. CHIMERE has developed diurnal factors for traffic emissions based on an objective analysis of NO_2 measurements in the different countries in Europe which improves ozone titration at night (Menut et al., 2012). Other reasons of the diurnal cycle in the model scores could also be errors in the diurnal cycle

of the boundary layer height and associated vertical diffusion. For instance, the boundary layer in the LOTOS-EUROS simulations is described with a single model level, with a diurnal variation in the boundary layer height obtained 3-hourly from the ECMWF forecasts. This differs from the description of vertical mixing in the other models and may be responsible for the low correlation feature at around 9 UTC. MATCH shows the largest diurnal variability that can be partly related to a combination of chemistry, deposition and the vertical resolution, where the latter is inherited from the IFS model with a rather shallow lowest model layer (~20m). The ozone depletion processes at the surface appears too strong and not enough compensated by the vertical diffusion. The MB is then more pronounced during night time, and a modification of the vertical diffusion has shown to improve MATCH skill.

Figure 6 also shows that there is generally a positive bias (both in MB and MNMB) of the ENSEMBLE for each of the 4 days of the forecast except around end afternoon when there is a slight ozone underestimation. The ENSEMBLE MB varies from -6 to 15.5 μg m^{-3}. This is consistent with the behaviour of the individual models, most of them having a positive bias on average. Only the MATCH model shows a negative bias (MB and MNMB) which has the same explanation as described above. The SILAM model has the highest positive ozone bias (MB and MNMB) on average. High ozone concentrations in SILAM are largely explained by too low dry deposition velocity over terrestrial areas, especially on the vegetated surfaces. The new scheme explicitly accounting for the leaf area index is being tested in pre-operational regime.

The normalized indicators (MNMB and FGE) of all 7 models vary from -0.45 to 0.45 and from 0.16 to 0.59, respectively. This means that all models perform fairly well for ozone in summer 2014. For the ENSEMBLE, MNMB and FGE are on average 0.14 (varying from -0.03 to 0.33) and 0.30 (varying from 0.16 to 0.45). These values, being well below 1, confirm the good skills of the ENSEMBLE. The ENSEMBLE correlation varies from 0.42 at night to 0.65 during daytime, consistently with the scores of the individual models.

The seven models show a fairly similar overall behaviour against observations because of their common framework (meteorology, chemical boundary conditions and emissions). Nevertheless, there are differences between ozone forecasted by each of the individual models because of their specificities (different chemistry schemes, different implementations for use of input data, different physical parameterizations). The ENSEMBLE gives generally better scores for ozone than any of the individual models.

In Section 3.3, we made a first investigation of the robustness of the ensemble median method with regard to the number of models available on a case study of one week. To go a step further, we ran a series of tests by removing one or more models in the calculation of the ensemble median over the three months of summer 2014. The removal is done randomly on each of the daily forecasts. Figure 7 shows the statistical results against observations for the ENSEMBLE (7 models) and the other ensemble medians calculated by removing randomly 1, 2, 3 or 4 models. For MB, MNMB and FGE, there is hardly any difference between all ensembles. Only RMSE and R (correlation) give significant changes. As expected, decreasing the number of models used in the ensemble tends to degrade its performances. Using 6 models gives RMSE and R close to the full ensemble based on 7 models. The scores for ensembles with 4 and 5 models are close to each other but are degraded compared to when 7 or 6 models are used. When only 3 models are used, RMSE and R are worse compared to the other configurations by ~0.5 $\mu g/m^3$ and ~0.05, respectively. This shows that, the multi-model ENSEMBLE at the end of MACC-II, which is based on the median of 7 models, is robust even if 2 to 3 models are unavailable. These results are consistent with the results discussed in Section 3.3 that were calculated on one week and with a different method for the model removal.

Figure 8 shows the ensemble scores for PM_{10} for the last winter (2013-2014) of MACC-II. Since there were much fewer observations available at 00UTC compared to other times of the day, the values given at the forecasts times of 0h, 24h, 48h, 72h and 96h show a specific behaviour that is not analysed since not typical. Among the 7 models, MATCH PM_{10} scores are the poorest for the period. This has been traced down to an error in the sea-salt emissions leading to too strong emissions and a coding error regarding summation of the various aerosol components that builds up PM_{10} in the model. Secondary organic aerosols are not yet included and there should be an underestimate, rather than an overestimate of PM_{10} by MATCH. The poor correlations in the period are partly related to a too strong signal from sea salt. The verification for 2015 shows clearly that correction of these errors has improved the simulation of PM_{10}. There is also a positive bias (~3.5 $\mu g\ m^{-3}$ on average for MB and 0.3 for MNMB) for CHIMERE. This could be due to specific set-up in CHIMERE to be more efficient in the detection of PM_{10} threshold exceedances during wintertime. It is achieved with a correction for lowering the wind over urban areas and with the modulation of the emissions from domestic heating to account for the impact of extremely low temperatures, occurring during cold surge for instance. The other extreme models are MOCAGE and SILAM that exhibits a

966 negative bias of about -6 μg m^{-3} on average for MB and -0.37 for MNMB. For MOCAGE,
967 this is due to the lack of secondary aerosols in the model. Although secondary aerosols are not
968 dominant in PM_{10} in winter, there is an expected contribution of sulfates mainly in Eastern
969 Europe. Substantial bias of SILAM PM_{10} is caused by the missing SOA. However, the model
970 showed the highest spatial correlation with the PM_{10} observations, which largely follows from
971 the detailed treatment of sea salt emission and transport. As a result, SILAM also showed
972 among the lowest RMSEs. LOTOS-EUROS, EURAD-IM, EMEP have a smaller negative
973 MB and NMNB. LOTOS-EUROS has an advanced treatment of the SIA fraction, but the
974 secondary organic aerosols (SOA) are not included yet, which explains part of the negative
975 bias. The bias in EMEP and EURAD-IM is relatively small as these two models include a
976 comprehensive treatment of SIA and SOA. The ENSEMBLE MB and MNMB both indicate a
977 low bias related to the fact that 5 of the 7 models have a negative bias. RMSE and FGE (Figs.
978 8c and 8d) are consistent with bias scores with largest values for MATCH and MOCAGE.
979 In Fig. 8, MB, MNMB, RMSE and FGE are best during daytime (generally around 06-07UTC
980 and 15UTC) with diurnal variations fairly similar for all models. This is related to the fact that
981 PM_{10} are dominated by primary anthropogenic emissions of black and organic carbon which
982 are prescribed in all model by the same TNO inventories and which have maxima in the
983 morning and in the afternoon. Worst MB, MNMB, RMSE and FGE are at night, as for ozone.
984 This may be linked to uncertainties in the boundary layer height at night, in vertical diffusion
985 and/or to an underestimation of emissions. The diurnal cycle is less marked in the correlation
986 but there is a significant day-to-day decrease of skills. As for ozone, this decrease is likely
987 linked to a decrease of the meteorological forecast skills with time which affects more the
988 correlation of pollutants than the other statistical indicators. Correlation values are fairly low,
989 a bit higher than 0.4 at maximum. This is due to the lack of certain types of aerosols (SIA
990 and/or SOA) in some models but also likely to uncertainties in the diurnal cycle of the
991 anthropogenic emissions prescribed in the models and of the boundary layer height and
992 vertical diffusion. The important contribution of traffic and residential heating to the
993 anthropogenic emissions of aerosols in Europe is generally modeled as two fixed peaks that
994 do not fully take into account the differences in habits between the countries in Europe. Also,
995 sea salts contribute to PM_{10} on the Western side of Europe with emissions and scavenging
996 depending closely to meteorological conditions and therefore directly affected by
997 meteorological uncertainties.
998 The ENSEMBLE scores are best compared to the 7 individual models for RMSE and FGE.
999 For MB and MNMB, EURAD-IM and EMEP models perform better than the ENSEMBLE.

This shows that there are compensating positive/negative biases in EURAD-IM and EMEP that are removed when RMSE and FGE scores are considered. The ENSEMBLE correlation is higher than the other models except SILAM.

Figures 6 and 8 show that the seven forecasts on which the ENSEMBLE is calculated are less skillful in modeling the aerosols than ozone. This is a common feature of most chemistry models since there are still large uncertainties on primary aerosol emissions and processes of production and evolution of secondary aerosols, particularly of secondary organic aerosols. Moreover, because of the operational context of MACC-II production, the seven forecasts models are optimized to run in short times. This constrains the level of detail of aerosol processes that can be afforded.

3.5 Example of the specific evaluation for the Mediterranean area

Within the European continent, the Mediterranean area is characterized by special features - high emission densities due to concentration of human activities in surrounding coastal areas, intense photochemistry, high background pollution, small scale meteorology that make air quality forecasting specially challenging. This is why work has been specifically carried out to evaluate the seven models and the ENSEMBLE in this region. This is complementary to the systematic daily and seasonal evaluation performed over the whole European continent. Its aim is not about scoring the system but on a better scientific understanding of the behaviour of the seven models and the ENSEMBLE in the Mediterranean region. This work is based, firstly, on two high resolution models run daily over eastern (Greece) Mediterranean and western (Spain) areas and surface station measurements that are not used in the operational MACC evaluation and, secondly, on scientific analyses of case studies.

For the Eastern Mediterranean area, the LAP-AUTH forecasting system is run daily. It consists of the Weather Research and Forecasting mesoscale meteorological model (WRF version 3.2) (Skamarock et al., 2008) and the chemistry transport model Comprehensive Air quality Model with extensions (CAMx version 5.30) (ENVIRON, 2010). The anthropogenic emission data, used as CAMx input data, are from Kuenen et al. (2014) for the reference year 2009. Anthropogenic emissions data are temporally processed using the Model for the Spatial and tEmporal diStribution of emissionS (MOSESS) (Markakis et al., 2013). The emissions originating from natural sources are calculated with the use of the emission model namely NEMO (Natural Emission MOdel) (Markakis et al. 2009). Wind erosion dust, sea salt and biogenic NMVOCs emissions are calculated using the WRF model meteorology. The air

quality forecasting system derives meteorological initial and boundary conditions from the operational 12:00 UTC forecast of ECMWF while chemical boundary conditions derived from the IFS–MOZART global model forecast and replaced by C-IFS from September 2014. The domain of the WRF - CAMx implementation is the South-East Europe/Eastern Mediterranean region from 18^{o}N-30^{o} N and 34.9^{o}E–44.5E. The grid resolution is 10 x 10 km^{2}. The air quality modelling system runs on a daily basis in order to produce 72-hours air quality forecasts. For the verification, the WRF-CAMx, the ENSEMBLE and the seven models are compared with available air quality data from the GMEECC (Greek Ministry of Environment Energy and Climatic Change) air pollution monitoring network as well as from the background station of Finokalia, operated by the University of Crete (Greece).

AEMET runs a version of the MOCAGE (Josse et al. 2004) model at 0.05º horizontal resolution in the Western Mediterranean coast, daily up to 48h using the ENSEMBLE forecasts as chemical lateral boundary conditions. Meteorological forcings for the high resolution domain come from operational HIRLAM run every 6 hours at AEMET (Navascues et al. 2013). Emissions over land in this domain come from the GEMS-TNO inventory (Visschedijk et al, 2007). The domain is 44ºN-36ºN-5ºW-5ºE. The ENSEMBLE has been compared to the AEMET forecasts and to observations from EMEP/GAW Spanish stations and from different local and regional Air Quality Monitoring networks. From these high resolution daily forecasts, a collection of case studies in which high resolution could have been an advantage, has been selected and analysed. These comparisons show the high variability of results between model forecasts depending on the location, time and day, whereas, sometimes, model forecast agreement is quite noticeable.

We are presenting here a brief summary of the analysis of the case study that occurred between the 15th and the 18th of July 2013, when high values of ozone were measured in many Spanish Air Quality Monitoring Stations due to very strong solar radiation and high temperatures together with persistent anticyclonic conditions and very weak pressure gradients. Ozone concentrations at surface above 140 μg/m^{3} were not rare at the stations used in this period and values above 120 μg/m^{3} were common. Figure 9 shows two maps with the 18th July 2013 ENSEMBLE and AEMET model at H+18 forecasts and the observations over-plotted using the same colour intervals. The ENSEMBLE forecasts generally fit well to the measurements. The main characteristic of the ENSEMBLE forecasts (left) is that it is too smooth to capture all the small scale features occurring in reality because of its horizontal resolution (~15 km). As an example, we can look at Fig. 9 in which the Madrid area has been

magnified to observe how ozone values between 100 and 160 μg/m^3 were measured by different Air Quality Networks (belonging to Madrid Regional Authorities and Madrid City Council) whereas in the ENSEMBLE forecasts all the concentrations are lying in the 100-120 μg/m^3 interval. In the same period, the AEMET forecasts provides values in this area with a higher spread, between 100 and 160 μg/m^3 which fits better to observations. Something similar can be observed in the Eastern Spain area, also magnified in the same figure.

Illustrations of the results of ENSEMBLE and AEMET models compared to three EMEP stations are given in Figs. 10 to 12 for ozone during summer. For Cap de Creus (Fig. 10), there is a good agreement between observations and models, but the two models have a wider diurnal cycle in concentrations. This behaviour can be related to the local dynamics. The area is located in a strong wind zone on the North-East coast of Spain. Therefore, ozone formed in this area can be transported rapidly, prohibiting ozone accumulation and leading to a smoother diurnal cycle than in the models that are not able to represent this local effect. For Mahon (Fig. 11), both models fit fairly well the observations but observations have generally a wider diurnal cycle in concentrations, contrarily to Cap de Creus. Mahon station is located in the small island of Menorca in the Balearic Archipelago. It is sometimes exposed to the pollution produced by ships entering the port early in the morning, leading to high NOx conditions and low ozone. This could explain the observed decrease of ozone at this time. This local effect is not captured by the two models. San Pablo de Montes measurements (Fig. 12) show a different behaviour with generally higher concentrations than the ENSEMBLE and AEMET models. The discrepancy is particularly important during July. This can be explained by an underestimation of the local isoprene emissions in the two models. Isoprene concentrations measured at San Pablo de los Montes exhibit higher values than other sites in the same area because of the oak vegetation surrounding the station.

Overall, the quality of the ENSEMBLE forecasts is generally good and the verification scores of the forecasts calculated for the whole period of the project show, most of the time, better results for the ENSEMBLE than for the AEMET forecasts. The limitations of the verification carried out (only the 7 EMEP background air quality stations within the domain have been considered) and the different high resolution emission inventories used in AEMET and ENSEMBLE can be part of the reason for these different results.

Another product we have started to generate at the end of the project is the behaviour of forecasts of the seven models together with the ENSEMBLE and the AEMET forecasts against observations from the EMEP Air Quality Network. An example is presented in Fig.

13. In this figure, we can see the ozone forecasts at ES10 station which is located at Cabo de Creus in the Northeastern corner of Spain (42.32N, 3.32 E). We observe that the spread between the seven model forecasts in the H+24 to H+48 forecast period from the 9th April 2014 is fairly low with most of the members producing similar forecasts. It changes quickly on the next day at the same place with the seven models providing very different concentrations leading to a high spread. We have also observed differences in the spread of the members at other locations on the same day and forecast time. More generally this pattern with very different spreads (ranging from low to high) depends on the case studies: day, time period and location. The analysis of the spread between different model forecasts in the same period can help modellers to understand how their models behave in the Mediterranean area.

4. Conclusion and future developments

In this paper, we give an overview of the current state and performances of the forecasting system for European air quality that was put in place in the framework of MACC project and continued during MACC-II project and now in the MACC-III project. Its strength comes from the fact that it is based on an ensemble of seven state-of-the-art chemistry-transport models (CHIMERE, EMEP, EURAD-IM, LOTOS-EUROS, MOCAGE, MATCH, SILAM) that are developed and run by recognized institutes in Europe. It also relies on good quality inputs for meteorological forcings, emissions and chemical boundary conditions. It provides daily 4-days forecasts for 6 major pollutants (O_3, NO_2, SO_2, CO, PM_{10} and $PM_{2.5}$) and birch pollen during pollen season, and also additional species for downscaling air quality modeling purposes. The production also includes hourly analysis for the previous day. Daily statistical performances of the forecasts against available European air quality monitoring station are processed on daily, weekly and 3 monthly bases, giving an objective assessment of the products to users. They are also used to monitor the seasonal and yearly evolutions of the forecast scores.

Because of the resolution of the seven models (10 to 20 km), this system is not designed and do not attempt to forecast very local concentrations but large scale phenomena and background air pollution. The ENSEMBLE has the capability to forecast pollution episodes at the regional scale as illustrated over the period from the 10th to the 13th of June 2014. On a seasonal basis, the 7 models show good statistical performances for ozone in summer 2014 and the ensemble median outperforms any of the individual models. The normalized indicators, that are less sensitive to outliers than MB and RMSE, are low, varying for the

ENSEMBLE from -0.03 to 0.33 for MNMB and from 0.16 to 0.45 for FGE. The diurnal ozone peak is underestimated by the ENSEMBLE by about 4 μg m^{-3} on average during summer 2014. The underestimation is larger during ozone episodes, such as during 9-15 June 2014, when the ENSEMBLE underestimates ozone daily maxima on average by about 10 μg m^{-3}. Comparing locally to surface station measurements within the pollution episode areas, the ENSEMBLE low bias is often between 30 and 50 μg m^{-3} but one of the models is often close to the observed values. For PM_{10}, there is a negative bias of the ENSEMBLE with MB ~ -4.5 mg m-3 and MNMB ~ -0.1, on average. The ENSEMBLE FGE is larger than for ozone (~0.52 on average for PM_{10} and 0.30 for ozone) and the correlation is lower (~0.35 on average for PM_{10} and 0.54 for ozone). There is a large variability of the statistical indicators of the 7 models for the last winter of MACC-II period (winter 2013-2014). This is related to different levels of complexity in the representation of aerosols in the models. PMs are regulatory pollutants that are difficult to forecast mainly because of uncertainties in primary aerosol emissions, our partial knowledge on secondary organic aerosol processes and the constraint of timely production that prevents using very sophisticated representations of secondary aerosols. A possibility of improvement of the ensemble median performances at low cost could be to remove the bias of the individual models before the ensemble median calculation. To complement the statistical evaluation done over the whole European domain, a scientific evaluation of the seven models and of the ENSEMBLE is also done for the Mediterranean region because of its specificities (emissions, population, topography, meteorology, photochemistry). Another important point to note is that major efforts have been put during MACC-II towards the full operationalisation of the system in order to improve its robustness.

The regional air quality production was extended during MACC-II and further developments are underway to improve the quality, the variety and the timeliness of its products based on users' feedbacks. In the very short term, the ENSEMBLE analysis that is only provided for ozone will be extended to NO_2 from January 2015 and verification statistics with independent data will be produced. It is also planned to shift the ENSEMBLE analysis production time earlier, at 11UTC from early 2015 following the users' recommendation. One planned change in the mid-term will be to have all individual models run at a ~10km horizontal resolution. This should improve the performances of the system compared to observations. Also the regional production benefits and will continue to benefit from the evolutions and improvements of the global production such as the use of the newly operated C-IFS (fully coupled chemistry to the IFS meteorological model) since September 2014 for regional

boundary conditions for chemical species and aerosols. In parallel, a dedicated fire emission product for regional forecast purposes, available earlier than the current operational product, is progressively implemented in the seven models and its usefulness will be assessed. Product evaluation is done on the basis of the available NRT measurements from the European AQ monitoring network. Stations used are selected to be as representative as possible of the model horizontal resolution, by retaining only classes 1 to 5 from the Joly and Peuch (2012) classification. There is ongoing work to improve the station selection, still based on Joly and Peuch's classification, by determining the best class ranges to be used individually for each of the 6 pollutants (O_3, NO_2, SO_2, CO, PM_{10}, $PM_{2.5}$) based on pollutant lifetime.

Continuous research is pursued to improve the seven individual models and their assimilation systems. In particular, there is an important effort on the use of new satellite data or combinations of satellite data with surface measurements in the assimilation systems. Also, there is on-going work on ensemble methods in order to extract as much value as possible from the seven model forecasts. Alternative methods to the median are currently tested: application of weights on the individual models at each grid point related to the performances from the day before or spectral decomposition (Galmarini et al. 2013). The results of these alternative methods applied to the MACC-II multi-model ensemble will be the subject of a forthcoming paper. Another goal in MACC-II was the start of research and developments for the modelling of CO_2 in the regional models in view of potential future high-resolution surface CO_2 flux inversion products over Europe. This work will be pursued.

In the next few years, the availability of more daily European surface observations, in a wider European area (i.e. from more countries) and at earlier time is foreseen. More data on a wider area would improve the strength of the statistical product evaluation. The continuous improvement of the quality of the surface monitoring data is also important for performance evaluation. Earlier availability of the surface station data would give the opportunity of an earlier production of the analyses with the goal of using the analyses as the initial state for the forecasts.

Other studies will be conducted on the possibility to provide complementary indicators such as the exceedences in ozone or PM_{10}. In the future, the production could be extended to other types of pollens than birch. There are currently some developments to test olive, grass and ambrosia pollens based on work done at the Finnish Meteorological Institute. Also, the possibility to produce additional species will be considered for users running forecast systems

at finer scales than the MACC-II system, such as the concentrations of different types of aerosols.

Appendix: Statistical indicators

The forecast performances are measured using five statistical indicators: the mean bias, the root mean square error, the modified normalized mean bias, the fractional gross error and the correlation.

The mean bias captures the average deviations between two datasets and is defined as:

$$MB = \frac{1}{N}\sum_{i}(f_i - o_i)$$

Where f_i and o_i are the forecast value at the observation location and the observation value, respectively.

The root mean square error combines the spread of individual error and is defined as:

$$RMSE = \sqrt{\frac{1}{N}\sum_{i}(f_i - o_i)^2}$$

It should be noted that the RMSE is strongly dominated by the largest values, due to the squaring operation. Especially in cases where prominent outliers occur, the usefulness of the RMSE is questionable and the interpretation becomes more difficult. MB and RMSE are not dimensionless variables, but have the same dimension as the modelled/observed quantity and requires knowledge of typical mean values. By scaling the MB and RMSE to the observations these metrics can be made relative, dimensionless, and hence more appropriate for use as a score. This is relevant when comparing bias and RMSE of atmospheric species whose concentrations can vary by orders of magnitude. This is why the modified normalized mean bias (MNMB) and the fractional gross error (FGE) are also used. MNMB is defined as:

$$MNMB = \frac{2}{N}\sum_{i}\left(\frac{f_i - o_i}{f_i + o_i}\right)$$

This gives a measure of forecast bias bounded by the values -2 to +2. It performs symmetrically with respect to under and over-prediction of the observations, which is a desirable feature.

FGE is defined as:

$$FGE = \frac{2}{N}\sum_i \left|\frac{f_i - o_i}{f_i + o_i}\right|$$

FGE gives a measure of the overall forecast error. This is proposed in addition to the more traditional RMSE, because due to the squaring procedure the RMSE gives the largest weight to the (possibly spurious) largest observations. FGE is bounded between 0 and 2.

In addition, the correlation coefficient is needed to indicate the extent to which patterns in the forecast match those in the observations. The correlation coefficient R between the forecast and observed values is defined as:

$$R = \frac{\frac{1}{N}\sum_i (f_i - \overline{f})(o_i - \overline{o})}{\sigma_f \sigma_o}$$

where $\overline{f}$ and $\overline{o}$ are the mean values of the forecast and observed values and σ_f and σ_o are the corresponding standard deviations. The correlation coefficient has a maximum value of unity when, for each observation site, $(f_i - \overline{f}) = c(o_i - \overline{o})$, where c is a positive constant. In this case the two datasets have the same pattern of variation but are not identical unless c=1 for all sites.

Acknowledgements

This study was funded by the European Commission under the EU Seventh Research Framework Programme (grant agreement no. 283576, MACC II). In-situ air quality data were provided by the European Environment Agency. Additional financial support at national level was given by the French Ministère de l'écologie, du développement durable et de l'énergie through the ADONISS project. This work was granted access to the HPC resources of CCRT under the allocation 2013-6695 made by GENCI (Grand Equipement National de Calcul Intensif). IASI has been developed and built under the responsibility of the Centre National d'Etudes Spatiales (CNES, France). Developments of SILAM system were supported by projects ASTREX and IS4FIRES of Academy of Finland. NO_2 column retrievals from AURA/OMI and METOP/GOME-2, and CO profiles from TERRA/MOPITT have been used for assimilation in some of the individual models.

References

Ackermann, I.J., Hass, H., Memmesheimer, M., Ebel, A., Binkowski, F.S., and Shankar, U.: Modal aerosol dynamics model for Europe: Development and first applications, Atmos. Environ., 32, 2981-2999, 1998.

Alfaro, S.C., and Gomes, L.: Modeling mineral aerosol production by wind erosion: Emission intensities and aerosol size distribution in source areas, J. Geophys. Res., 106, 18,075-18,084, 2001.

Andersson-Sköld, Y., and Simpson, D.: Comparison of the chemical schemes of the EMEP MSC-W and IVL photochemical trajectory models, Atmospheric Environment, 33, 1111–1129, 1999.

Andersson, C., Langner, J., and Bergström, R.: Interannual variation and trends in air pollution over Europe due to climat variability during 1958-2001 simulated with a regional CTM coupled to the ERA40 reanalysis. Tellus 59B, 77-98, 2007.

Andersson, C., Bergström, R., Bennet, C., Robertson, L., Thomas, M., Korhonen, H., Lehtinen, K.E.J. and Kokkola, H.: MATCH-SALSA – Multi-scale Atmospheric Transport and Chemistry model coupled to the SALSA aerosol microphysics model – Part 1: model description and evaluation. Geosci. Model Dev., 8, 171-189, 2015.

Baklanov, A., Schlünzen, K., Suppan, P., Baldasano, J., Brunner, D., Aksoyoglu, S., Carmichael, G., Douros, J., Flemming, J., Forkel, R., Galmarini, S., Gauss, M., Grell, G., Hirtl, M., Joffre, S., Jorba, O., Kaas, E., Kaasik, M., Kallos, G., Kong, X., Korsholm, U., Kurganskiy, A., Kushta, J., Lohmann, U., Mahura, A., Manders-Groot, A., Maurizi, A., Moussiopoulos, N., Rao, S. T., Savage, N., Seigneur, C., Sokhi, R. S., Solazzo, E., Solomos, S., Sørensen, B., Tsegas, G., Vignati, E., Vogel, B., and Zhang, Y.: Online coupled regional meteorology chemistry models in Europe: current status and prospects, Atmos. Chem. Phys., 14, 317-398, doi:10.5194/acp-14-317-2014, 2014.

Barbu, A.L., Segers, A.J., Schaap, M., Heemink, A.W., and Builtjes, P.J.H.: A multi-component data assimilation experiment directed to sulphur dioxide and sulphate over Europe, Atmos. Env., 43(9), 1622-1631, 10.1016/j.atmosenv.2008.12.005, 2008.

Barré, J., El Amraoui, L., Ricaud, P., Lahoz, W. A., Attié, J.-L., Peuch, V.-H., Josse, B., and Marécal, V.: Diagnosing the transition layer at extratropical latitudes using MLS O_3 and MOPITT CO analyses Atmos. Chem. Phys., 13, 7225-7240, 2013.

1278 Barré, J., Peuch, V.-H., Lahoz, W. A., Attié, J.-L., Josse, B., Piacentini, A., Emerenko, M.,
1279 Dufour, G., Nédélec, P., von Clarmann, T., and El Amraoui, L.: Combined data assimilation
1280 of ozone tropospheric columns and stratospheric profiles in a high-resolution CTM. Q. J. Roy.
1281 Meteorol. Soc., 140, 966-981, doi:10.1002/qj.2176, 2014.

1282 Bechtold, P., Bazile, E., Guichard, F., Mascart, P., and Richard, E.: A mass-flux convection
1283 scheme for regional and global models, Q. J. R. Meteorol. Soc., 127, 869–886, 2001.

1284 Beekmann, M., and Vautard, R.: A modelling study of photochemical regimes over Europe:
1285 robustness and variability, Atmos. Chem. Phys., 10, 10067-10084, 2010.

1286 Benedetti, A., Morcrette, J.-J., Boucher, O., Dethof, A., Engelen, R. J., Fisher, M., Flentje,
1287 H., Huneeus, N., Jones, L., Kaiser, J. W., Kinne, S., Mangold, A., Razinger, M., Simmons,
1288 A. J., and Suttie, M.: Aerosol analysis and forecast in the European Centre for Medium-Range
1289 Weather Forecasts Integrated Forecast System. 2. Data assimilation: J. Geophys. Res., 114 ,
1290 D13205, doi:10.1029/2008JD011115, 2009.

1291 Bergström, R., Denier van der Gon, H. A. C., Prévôt, A. S. H., Yttri, K. E., and Simpson, D.:
1292 Modelling of organic aerosols over Europe (2002–2007) using a volatility basis set (VBS)
1293 framework: application of different assumptions regarding the formation of secondary organic
1294 aerosol, Atmos. Chem. Phys., 12, 8499–8527, doi:10.5194/acp-12-8499-2012, 2012.

1295 Bessagnet, B., Hodzic, A., Vautard, R., Beekmann, M., Cheinet, S., Honoré, C., Liousse, C.,
1296 and Rouil, L.: Aerosol modeling with CHIMERE: preliminary evaluation at the continental
1297 scale, Atmospheric Environment, 38, 2803--2817, 2004.

1298 Bessagnet, B., Menut, L., Curci, G., Hodzic, A., Guillaume, B., Liousse, C., Moukhtar, S.,
1299 Pun, B., Seigneur, C., and Schulz, M.: Regional modeling of carbonaceous aerosols over
1300 Europe - Focus on Secondary Organic Aerosols, Journal of of Atmospheric Chemistry, 61,
1301 175-202, 2009.

1302 Bott, A.: A positive definite advection scheme obtained by nonlinear renormalization of the
1303 advective fluxes, Mon. Weather Rev., 117, 1006-1016, 1989.

1304 Bousserez, N., Attié, J.-L., Peuch, V.-H., Michou, M., Pfister, G., Edwards, D., Avery, M.,
1305 Sachse, G., Browell, E., and Ferrare, E.: Evaluation of MOCAGE chemistry and transport
1306 model during the ICARTT/ITOP experiment, J. Geophys. Res., 112 (D120S42), doi: 10.1029/
1307 2006JD007595, 2007.

1308 Burridge, D.M., and Gadd, A. J.: The Meteorological Office Operational 10-level numerical
1309 weather prediction model, Sci. Pap., 34, UK Meteorological Office, 1977.

1310 Carter, W.P.L: Condensed atmospheric photo oxidation mechanism for isoprene. Atmos.
1311 Environ. 30, 4275-4290, 1996.

1312 Colette, A., Granier, C., Hodnebrog, O., Jakobs, H., Maurizi, A., Nyiri, A., Bessagnet, B.,
1313 D'Angiola, A., D'Isidoro, M., Gauss, M., Meleux, F., Memmesheimer, M., Mieville, A.,
1314 Rouil, L., Russo, F., Solberg, S., Stordal, F., and Tampieri, F.: Air quality trends in Europe
1315 over the past decade: a first multi-model assessment, Atmos. Chem. Phys., 11, 11,657-11,678,
1316 10.5194/acp-11-11657-2011, 2011.

1317 Curier, R.L., Timmermans, R., Calabretta-Jongen, S., Eskes, H., Segers, A., Swart, D., and
1318 Schaap, M.: Improving ozone forecasts over Europe by synergistic use of the LOTOS-
1319 EUROS chemical transport model and in-situ measurements, Atmos. Env., 60, 217-226,
1320 doi:10.1016/j.atmosenv.2012.06.017, 2012.

1321 Cuvelier, C., Thunis, P., Vautard, R., Amann, M., Bessagnet B., Bedogni, M., Berkowicz, R.,
1322 Brandt, J., Brocheton, F., Builtjes, P., Coppalle, A., Denby, B., Douros, G., Graf, A.,
1323 Hellmuth, O., Honoré, C., Hodzic, A., Jonson, J., Kerschbaumer, A., de Leeuw, F., Minguzzi,
1324 E., Moussiopoulos, N., Pertot, C., Pirovano, G., Rouil, L., Schaap, M., Stern, R., Tarrason, L.,
1325 Vignati, E., Volta, M., White, L., Wind, P., and Zuber A.: CityDelta: A model
1326 intercomparison study to explore the impact of emission reductions in European cities in
1327 2010, Atmos. Env., 41, 189-207, 10.1016/j.atmosenv.2006.07.036, 2007.

1328 Delle Monache, L., Deng, X., Zhou, Y., and Stull, R.: Ozone ensemble forecasts: 1. A new
1329 ensemble design, J. Geophys. Res., 111, D05307, doi:10.1029/2005JD006310, 2006.

1330 De Ruyter de Wildt, M., Eskes, H., Manders, A., Sauter, F., Schaap, M., Swart, D., and van
1331 Velthoven, P.: Six-Day PM10 Air Quality Forecasts For The Netherlands With The
1332 Chemistry Transport Model Lotos-Euros,, Atmos. Env., 45, p5586-5594,,
1333 doi:10.1016/j.atmosenv.2011.04.049, 2011.

1334 Dufour, A., Amodei, M., Ancellet, G., and Peuch, V.-H.: Observed and modelled "chemical
1335 weather" during ESCOMPTE, Atmos. Res., 74 (1-4), 161-189, 2004.

1336 Ebel, A., Jakobs, H., Memmesheimer, M., Elben, H., and Feldmann, H.: Numerical forecast
1337 of air pollution: advances and problems, vol. Advances in Air Pollution Modeling for
1338 Environmental Security, Springer, doi:10.1007/1-4020-3351-6_14, 2005.

El Amraoui, L., Peuch, V.-H., Ricaud, P., Massart, S., Semane, N., Teyssèdre, H., and Karcher, F.: Ozone loss in the 2002–2003 Arctic vortex deduced from the assimilation of Odin/SMR O3 and N2O measurements: N2O as a dynamical tracer. Q. J. R. Meteorol. Soc., 134(630), 217–228. doi:10.1002/qj.191, 2008.

Elbern, H., Strunk, A., Schmidt, P., and Talagrand, O.: Emission rate and chemical state estimation by 4-dimensional variational inversion, Atmos. Chem. Phys., 7, 3749-3769, 2007.

Elbern, H., Strunk, A., Friese, E., and Nieradzik, L.: Assessment of Source/Receptor Relations by Inverse Modelling and Chemical Data Assimilation, in Persistent Pollution Past, Present and Future School of Environmental Research - Helmholtz-Zentrum Geesthacht, Quante, M.; Ebinghaus, R.; Flöser, G. (Eds.) 1st Edition, ISBN 978-3-642-17420-9, 2011.

Emili, E., Barret, B., Massart, S., Le Flochmoen, E., Piacentini, A., El Amraoui, L., Pannekoucke, O., and Cariolle, D. : Combined assimilation of IASI and MLS observations to constrain tropospheric and stratospheric ozone in a global chemical transport model, Atmos. Chem. Phys., 14, 177-198, 2014.

ENVIRON: User's guide CAMx - Comprehensive Air Quality Model with extensions, Version 5.30, ENVIRON International Corporation, 415.899.0700, December 2010, 2010.

Fagerli, H. and Aas, W.: Trends of nitrogen in air and precipitation: Model results and observations at EMEP sites in Europe, 1980-2003, Environ. Poll., 154, 448–461, 2008.

Flemming, J., Inness, A., Flentje, H., Huijnen, V., Moinat, P., Schultz, M. G., and Stein, O.: Coupling global chemistry transport models to ECMWF's integrated forecast system, Geosci. Model Dev., 2, 253-265, 2009.

Flemming, J., Huijnen, V., Arteta, J., Bechtold, P., Beljaars, A., Blechschmidt, A.-M., Josse, B., Diamantakis, M., Engelen, R. J., Gaudel, A., Inness, A., Jones, L., Katragkou, E., Marécal, V., Peuch, V.-H., Richter, A., Schultz, M. G., Stein, O., and Tsikerdekis, A.: Tropospheric chemistry in the integrated forecasting system of ECMWF, Geosci. Model Dev., 7, 7733-7803, 2014.

Friese, E., and Ebel, A.: Temperature dependent thermodynamic model of the system H^+-NH_4^+-Na^+-SO_4^{2-}-NO_3^--Cl^--H_2O, J. Phys. Chem. A., 114, 11595-11631, 2010.

Foltescu, V.L., Pryor, C.S., and Bennet, C.: Sea salt generation, dispersion, and removal on the regional scale. Atmos Environ 39, 2113-2133, 2005.

1369 Fountoukis, C., and Nenes, A.: ISORROPIA II: a computationally efficient thermodynamic
1370 equilibrium model for K+-Ca2+-Mg2+-NH4+-Na+-SO42−-NO3−-Cl−-H2O aerosols, Atmos.
1371 Chem. Phys., 7, 4639–4659, doi:10.5194/acp-7-4639-2007, 2007.

1372 Fuhrer, J., and Booker, F.: Ecological issues related to ozone: agricultural issues, Environ.
1373 Int., 29, 141–154, 2003.

1374 Galmarini, S., Kioutsioukis, I, and Solazzo, E.: E pluribus unum: ensemble air quality
1375 predictions, Atmos. Chem. Phys., 13, 7153-7182, 2013.

1376 Galperin, M. V.: The Approaches to Correct Computation of Airborne Pollution Advection,
1377 in: Problems of Ecological Monitoring and Ecosystem Modelling. XVII (in Russian).
1378 Gidrometeoizdat, St.Petersburg, pp. 54–68, 2000.

1379 Gaubert, B., Coman, A., Foret, G., Meleux, F., Ung, A., Rouil, L., Ionescu, A., Candau, Y.,
1380 and Beekmann, M.: Regional scale ozone data assimilation using an ensemble Kalman filter
1381 and the CHIMERE chemical transport model, Geosci. Model Dev., 7, 283–302, 2014.

1382 Geer, A.J. , Lahoz, W.A., Bekki, S., Bormann, N., Errera, Q., Eskes, H.J., Fonteyn, D.,
1383 Jackson, D.R., Juckes, M.N., Massart, S., Peuch, V.-H., Rharmili, S., and Segers, A.: The
1384 ASSET intercomparison of ozone analyses : method and first results, Atmos. Chem. Phys., 6,
1385 5445-5474, 2006.

1386 Geiger, H., Barnes, I. , Bejan, I., Benter, T., and Spttler, M.: The tropospheric degradation of
1387 isoprene: an updated module for the regional atmospheric chemistry mechanism, Atmos.
1388 Env., 37, 1503-1519, 2003.

1389 Genberg, J., Denier van der Gon, H. A. C., Simpson, D., Swietlicki, E., Areskoug, H.,
1390 Beddows, D., Ceburnis, D., Fiebig, M., Hansson, H. C., Harrison, R. M., Jennings, S. G.,
1391 Saarikoski, S., Spindler, G., Visschedijk, A. J. H., Wiedensohler, A., Yttri, K. E., and
1392 Bergström, R.: Light-absorbing carbon in Europe – measurement and modelling, with a focus
1393 on residential wood combustion emissions, Atmos. Chem. Phys., 13, 8719–8738,
1394 doi:10.5194/acp-13-8719-2013, 2013.

1395 Giglio, L., Randerson, J. T., van der Werf, G. R., Kasibhatla, P. S., Collatz, G. J., Morton, D.
1396 C., and DeFries, R. S.: Assessing variability and long-term trends in burned area by
1397 mergingmultiple satellite fire products, Biogeosciences, 7, 1171–1186, doi: 10.5194/bg-7-
1398 1171-2010, 2010.

1399 Giorgi, F., and Chameides, W. L.: Rainout lifetimes of highly soluble aerosols and gases as
1400 inferred from simulations with a general circulation model, J. Geophys. Res.: Atmospheres,
1401 91, 14 367–14 376, 1986.

1402 Guenther, A. B., Hewitt, C. N., Erickson, D., Fall, R., Geron, C., Graedel, T., Harley, P.,
1403 Klinger, L., Lerdau, M., Mckay, W. A., Pierce, T., Scholes, B., Steinbrecher, R., Tallamraju,
1404 R., Taylor, J., and Zimmerman, P.: A global model of natural volatile compound emissions, J.
1405 Geophys. Res., 100, 8873–8892, doi:10.1029/94JD02950, 1995.

1406 Guenther, A., Karl, T., Harley, P., Wiedinmyer, C., Palmer, P., and Geron, C.: Estimates of
1407 global terrestrial isoprene emissions using MEGAN (Model of Emissions of Gases and
1408 Aerosols from Nature), Atmos. Chem. Phys., 6, 3181--3210, 2006.

1409 Guenther, A. B., Jiang, X., Heald, C.L., Sakulyanontvittaya, T., Duhl, T., Emmons, L.K., and
1410 Wang, X.: The Model of Emissions of Gases and Aerosols from Nature version 2.1
1411 (MEGAN2.1). An extended and updated framework for modeling biogenic emissions. Geosci.
1412 Model Dev., 5, 1471-1492, 2012.

1413 Guenther, A. B., Zimmerman, P. R., Harley, P. C., Monson, R. K., and Fall, R.: Isoprene and
1414 Monoterpene Emission Rate Variability: Model Evaluations and Sensitivity Analyses, J.
1415 Geophys. Res., 98, dx.doi.org/10.1029/93JD00527, 1993.

1416 Guth, J., Josse, B., Marécal, V., and Joly, M.: Simulating Secondary Inorganic Aerosols
1417 using the Chemistry Transport Model MOCAGE, Geosci. Mod. Dev. Discuss., 8, 3593-3651,
1418 2015.

1419 Hass, H., Jakobs, H.J., and Memmesheimer, M.: Analysis of a regional model (EURAD) near
1420 surface gas concentration predictions using observations from networks, Met. Atmos. Phys.,
1421 57, 173-200, 1995.

1422 Heimann, M., and Keeling, C.D.: A three-dimensional model of CO_2 tramsport based on
1423 observed winds. Model description and simulated trace experiment. In aspects of Climate
1424 Variability in the Pacific and Western Americas (ed. D.H Peterson). American Geophysical
1425 Union, Washington, DC, pp. 237-275, 1989.

1426 Hollingsworth, A., Engelen, R.J., Textor, C., Benedetti, A., Boucher, O., Chevallier, F.,
1427 Dethof, A., Elbern, H., Eskes, H., Flemming, J., Granier, C., Kaiser, J.W., Morcrette, J.J.,
1428 Rayner, P., Peuch, V.H., Rouil, L., Schultz, M.G., and Simmons, A.J.: and The GEMS
1429 Consortium: Toward a Monitoring and Forecasting System For Atmospheric Composition:

1430 The GEMS Project. Bull. Amer. Meteor. Soc., 89, 11471164, doi:10.1175/2008BAMS2355.1,
1431 2008.

1432 Holtslag, A. A. M., and Moeng, C.-H.: Eddy diffusivity and countergradient transport in the
1433 convective atmospheric boundary layer. J. Atmos. Sci., 48, 1690-1700, 1991.

1434 Holtslag, A.A.M., and Nieuwstadt, F.T.M.: Scaling the atmospheric boundary layer,
1435 Boundary-Layer Met., 36, 201-209, 1986.

1436 Holtslag. A.A.M., Meigaard, E. van, and De Rooy, W.C: A comparison of boundary layer
1437 diffusion schemes in unstable conditions over land. Boundary Layer Met., 76, 69-95, 1995.

1438 Honoré, C., Rouil, L., Vautard, R., Beekmann, M., Bessagnet, B., Dufour, A., Elichegaray,
1439 C., Flaud, J.-M., Malherbe, L., Meleux, F., Menut, L., Martin, D., Peuch, A., Peuch, V.-H.,
1440 and Poisson, N.: Predictability of European air quality : Assessment of 3 years of operational
1441 forecasts and analyses by the PREV'AIR system, J. Geophys. Res., D113, D04301,
1442 doi:10.1029/2007JD008761, 2008.

1443 Huijnen, V., Williams, J. E., van Weele, M., van Noije, T. P. C., Krol, M. C., Dentener, F.,
1444 Segers, A., Houweling, S., Peters, W., de Laat, A. T. J., Boersma, K. F., Bergamaschi, P., van
1445 Velthoven, P. F. J., Le Sager, P., Eskes, H. J., Alkemade, F., Scheele, M. P., Nedelec, P., and
1446 Patz, H.-W.: The global chemistry transport model TM5: description and evaluation of the
1447 tropospheric chemistry version 3.0, Geosci. Model Dev., 3, 445-473, 2010.

1448 Inness, A., Baier, F., Benedetti, A., Bouarar, I., Chabrillat, S., Clark, H., Clerbaux, C.,
1449 Coheur, P., Engelen, R. J., Errera, Q., Flemming, J., George, M., Granier, C., Hadji-Lazaro,
1450 J., Huijnen, V., Hurtmans, D., Jones, L., Kaiser, J. W., Kapsomenakis, J., Lefever, K., Leitão,
1451 J., Razinger, M., Richter, A., Schultz, M. G., Simmons, A. J., Suttie, M., Stein, O., Thépaut,
1452 J.-N., Thouret, V., Vrekoussis, M., Zerefos, C., and the MACC team: The MACC reanalysis:
1453 an 8 yr data set of atmospheric composition, Atmos. Chem. Phys., 13, 4073-4109,
1454 doi:10.5194/acp-13-4073-2013, 2013.

1455 Jaumouillé, E., Massart, S., Piacentini, A., Cariolle, D., and Peuch, V.-H.: Impact of a time-
1456 dependent background error covariance matrix on air quality analysis, Geosci. Model
1457 Dev., 5, 1075-1090, 2012.

1458 Joly, M., and Peuch, V.-H.: Objective Classification of air quality monitoring sites over
1459 Europe, Atmos. Env., 47, 111-123, 2012.

1460 Jonson, J. E., Simpson, D., Fagerli, H., and Solberg, S.: Can we explain the trends in
1461 European ozone levels?, Atmos. Chem. Phys., 6, 51–66, doi:10.5194/acp-6-51-2006, 2006.

1462 Josse, B., Simon, P., and Peuch, V.-H.: Radon global simulations with the multiscale
1463 chemistry and transport model MOCAGE, Tellus B, 56, 339-356, 2004.

1464 Kahnert, M.: Variational data analysis of aerosol species in a regional CTM: background error
1465 covariance constraint and aerosol optical observation operators, Tellus, 60, 753–770,
1466 doi:10.1111/j.1600-0889.2008.00377.x, 2008.

1467 Kahnert, M.: On the observability of chemical and physical aerosol properties by optical
1468 observations: inverse modelling with variational data assimilation, Tellus B, 61, 747–755,
1469 doi:10.1111/j.1600-0889.2009.00436.x, 2009.

1470 Kaiser, J.W., Heil, A., Andreae, M. O, Benedetti, A., Chubarova, N., Jones, L., Morcrette, J.-
1471 J., Razinger, M., Schultz, M. G., Suttie, M. and van der Werf,G. R.: Biomass burning
1472 emissions estimated with a global fire assimilation system based on observed fire radiative
1473 power, Biogeosciences, 9, 527–554,doi:10.5194/bg-9-527-2012, 2012

1474 Kanakidou, M., Dameris, M., Elbern, H., Beekmann, M., Konovalov, I., Nieradzik, L.,
1475 Strunk, A., and Krol, M.: Synergistic use of retrieved trace constituents distributions and
1476 numerical modelling, in "The remote sensing of tropospheric composition from space", J.
1477 Burrows, U. Platt, P. Borrell (Eds.), Springer, doi 10.1007/978-3-642-14791-3, 2011.

1478 Kioutsioukis, I., and Galmarini, S.: *De praeceptis ferendis:* good practice in multi-model
1479 ensembles, Atmos. Chem. Phys., 14, 11791-11815, 2014.

1480 Köble, R., and Seufert, G.: Novel maps for forest tree species in Europe, in: Proceedings of
1481 the 8th European symposium on the physico-chemical behaviour of air pollutants:“a changing
1482 atmosphere, pp. 17–20, 2001.

1483 Kouznetsov, R. and Sofiev, M.: A methodology for evaluation of vertical dispersion and dry
1484 deposition of atmospheric aerosols, J. Geophys. Res., 117, D01202,
1485 doi:10.1029/2011JD016366, 2012.

1486 Kuenen, J. J. P., Denier van der Gon, H. A. C., Visschedijk, A., Van der Brugh, H., and Van
1487 Gijlswijk, R.: MACC European emission inventory for the years 2003-2007, TNO report
1488 TNO-060-UT-2011-00588, Utrecht, 2011.

1489 Kuenen, J. J. P., Visschedijk, A. J. H., Jozwicka, M., and Denier van der Gon, H. A. C.: TNO-
1490 MACC_II emission inventory: a multi-year (2003–2009) consistent high-resolution European
1491 emission inventory for air quality modelling, Atmos. Chem. Phys., 14, 10963-10976, 2014.

1492 Kukkonen, J., Olsson, T., Schultz, D. M., Baklanov, A., Klein, T., Miranda, A. I., Monteiro,
1493 A., Hirtl, M., Tarvainen, V., Boy, M., Peuch, V.-H., Poupkou, A., Kioutsioukis, I., Finardi, S.,
1494 Sofiev, M., Sokhi, R., Lehtinen, K. E. J., Karatzas, K., San José, R., Astitha, M., Kallos, G.,
1495 Schaap, M., Reimer, E., Jakobs, H., and K. Eben: A review of operational, regional-scale,
1496 chemical weather forecasting models in Europe , Atmos. Chem. Phys., 11, 1-87, 2012.

1497 Lacressonnière, G., Peuch, V.-H., Vautard, R., Arteta, J., Déqué, M., Josse, B., Marécal, V.,
1498 and Saint-Martin, D.: European air quality in the 2030s and 2050s: Impacts of global and
1499 regional emission trends and of climate change, Atmos. Env., 92, 348-358, 2014.

1500 Lahoz, W.A., Geer, A.J., Bekki, S., Bormann, N., Ceccherini, S., Elbern, H., Errera, Q.,
1501 Eskes, H.J., Fonteyn, D., Jackson, D.R., Khattatov, B., Massart, S., Peuch, V.-H., Rharmili,
1502 S., Ridolfi, M., Segers, A., Talagrand, O., Thornton, H.E., Vik, A.F., and Von Clarman T.:
1503 The Assimilation of Envisat data (ASSET) project, Atmos. Chem. Phys., 7, 1773-1796, 2007.

1504 Langner, J., Bergström, R., and Pleijel, K.: European scale modeling of sulphur, oxidized
1505 nitrogen and photochemical oxidants. Model dependent development av evaluation for the
1506 1994 growing season. SMHI report, RMK No. 82, Swedish Met. And Hydrol. Inst.,
1507 Norrköping, Sweden, 1998.

1508 Lefèvre, F., Brasseur, G. P., Folkins, I., Smith, A. K., and Simon, P.: Chemistry of the 1991–
1509 1992 stratospheric winter: Three-dimensional model simulations, J. Geophys. Res. :
1510 Atmospheres, 99, 8183–8195, 1994.

1511 Li, Y.P. Elbern, H., Liu, K.D., Friese, E., Kiendler-Scharr, A., Mentel, Th.F., and Wang, X.S.,
1512 Wahner, A., and Zhang, Y.H.: Updated aerosol module and its application to simulate
1513 secondary organic aerosols during IMPACT campaign May 2008, Atmos. Chem. Phys., 13,
1514 6289 - 6304, 2013, doi:10.5194/acp-13-6289-2013.

1515 Liu, D.C., and Nocedal, J.: On the limited memory BFGS method for large scale optimization,
1516 Math. Programming, 45, 503-528, 1989.

1517 Louis, J.-F.: A parametric model of vertical eddy fluxes in the atmosphere, Boundary-Layer
1518 Meteorology, 17, 187–202, 1979.

Madronich, S., and Weller, G.: Numerical integration errors in calculated tropospheric photodissociation rate coefficients, J. Atmos. Chem., 10, 289-300, 1990.

Mari, C., Jacob, D. J., and Bechtold, P.: Transport and scavenging of soluble gases in a deep convective cloud, J. Geophys. Res. : Atmospheres, 105, 22 255–22 267, 2000.

Markakis, K., Giannaros, T., Poupkou, A., Liora, N., Melas, D., Sofiev, M. and Soares, J.: Evaluating the impact of particle emissions from natural sources in the Balkan region, European Aerosol Conference 2009, 6-9 September 2009, Karlsruhe, Germany, 2009.

Markakis, K., Katragkou, E., Poupkou, A. and Melas, D.: "MOSESS: A new emission model for the compilation of model-ready emission inventories. Application in a coal mining area in Northern Greece", Environmental Modeling & Assessment, 18, pp. 509–521, 2013.

Martet, M., Peuch, V.-H., Laurent, B., Marticorena B., and Bergametti, G.: evaluation of long-range transport and deposition of desert dust with the CTM Mocage, Tellus, 61B, 449-463, 2009.

Massart, S., Clerbaux, C., Cariolle, D., Piacentini, A., Turquety, S., and Hadji-Lazaro, J.: First steps towards the assimilation of IASI ozone data into the MOCAGE-PALM system. Atmos. Chem. Phys., 9(14), 5073–5091. doi:10.5194/acp-9-5073-2009, 2009.

Memmesheimer, M., Friese, E., Ebel, A., Jakobs, H. J., Feldmann, H., Kessler, C., and Piekorz, G.: Long-term simulations of particulate matter in Europe on different scales using sequential nesting of a regional model, Int. J. Environm. and Pollution, 22, (1-2), 108-132, 2004.

Menut, L., and Bessagnet, B.: Atmospheric composition forecasting in Europe, Ann. Geophys. 28, 61-74, 2010.

Menut, L., Goussebaile, A., Bessagnet, B., Khvorostiyanov, D., Ung, A.: Impact of realistic hourly emissions profiles on modelled air pollutants concentrations, Atmos. Env., pp. 233-244, doi:10.1016/j.atmosenv.2011.11.057, 2012.

Menut L, Bessagnet, B., Khvorostyanov, D., Beekmann, M., Blond, N., Colette, A., Coll, I., Curci, G., Foret, G., Hodzic, A., Mailler, S., Meleux, F., Monge, J. L., Pison, I., Siour, G., Turquety, S., Valari, M., Vautard, R., and Vivanco, M.G.: CHIMERE 2013 a model for regional atmospheric composition modelling, Geosci. Model Dev., 6, 981-1028, doi:10.5194/gmd-6-981-2013, 2013.

1549 Menut L., Perez Garcia-Pando, C., Haustein, K., Bessagnet, B., Prigent, C., and Alfaro, S.:
1550 Relative impact of roughness and soil texture on mineral dust emission fluxes modeling, J.
1551 Geophys. Res.: Atmospheres, 118, 6505-6520, doi:10.1002/jgrd.50313, 2013.

1552 Monteiro, A., Ribeiro, I., Tchepel, O., Sá, E., Ferreira, J., Carvalho, A., Martins, V., Strunk,
1553 A., Galmarini, S., Elbern, H., Schaap, M., Builtjes, P., Miranda, A. I., and Borrego, C.: Bias
1554 Correction Techniques to Improve Air Quality Ensemble Predictions: Focus on O3 and PM
1555 Over Portugal, Environ. Model. Assess., 18, 533-546,doi:10.1007/s10666-013-9358-2, 2013.

1556 Monteiro, A., Strunk, A., Carvalho, A., Tchepel, O., Miranda, A. I., Borrego, C., Saavedra, S.,
1557 Rodriguez, A., Souto, J., Casares, J., Friese, E., and Elbern, H.: Investigating a very high
1558 ozone episode in a rural mountain site, Env. Pol., 162, 176-189, 2012.

1559 Morcrette, J.-J., Boucher, O., Jones, L., Salmond, D., Bechtold, P., Beljaars, A., Benedetti,
1560 A., Bonet, A., Kaiser, J. W., Razinger, M., Schulz, M., Serrar, S., Simmons, A. J., Sofiev, M.,
1561 Suttie, M., Tompkins, A. M., and Untch, A.: Aerosol analysis and forecast in the European
1562 Centre for Medium-Range Weather Forecasts Integrated Forecast System. 1. Forward
1563 modelling: J. Geophys. Res., 114 , D06206, doi:10.1029/2008JD011235, 2009.

1564 Navascues, B., Calvo, J., Morales, G., Santos, C., Callado, C., Cansado, A., Cuxart, J., Diez,
1565 M., del Rio, P., Escriba, P., Garcia-Colombo, O., García-Moya, J.A., Geijo, C., Gutierrez, E.,
1566 Hortal, M., Martinez, I., Orfila, B., Parodi, J.A., Rodriguez, E., Sánchez-Arriola, J., Santos-
1567 Atienza, I., Simarro, J.: Long term verification of HIRLAM and ECMWF forecasts over
1568 Southern Europe. History and perspectives of Numerical Weather Prediction at AEMET,
1569 Atmos. Res. 125-126, pp 20-33, doi:10.1016/j.atmosres.2013.01.010, 2013.

1570 Nho-Kim, E.-Y., Peuch, V.-H., and Oh, S. N.: Estimation of the global distribution of Black
1571 Carbon aerosols with MOCAGE, the CTM of Météo-France, J. Korean Meteor. Soc., 41(4),
1572 587-598, 2005.

1573 Nieradzik, L.P.: Application of a high dimensional model representation on the atmospheric
1574 aerosol module MADE of the EURAD-CTM, Master Thesis, Institut für Geophysik und
1575 Meteorologie der Universität zu Köln, 2005.

1576 Nocedal, J.: Updating quasi-Newton matrices with limited storage, Math. Comput., 35 (151),
1577 773-782, 1980.

1578 Parrish, D. F., and Derber, J. C.: The national meteorological center's spectral statistical-
1579 interpolation analysis system, Mon. Weather Rev., 120(8), 1747-1763, 1992.

1580 Petroff, A., and Zhang, L.: Development and application of a size-resolved particle dry
1581 deposition scheme for application in aerosol transport models, Geosci. Model Dev., 3, 753-
1582 769, doi: 10.5197/gmd-3-753-2010.

1583 Poupkou, A., Giannaros, T., Markakis, K., Kioutsioukis, I., Curci, G., Melas, D., and Zerefos,
1584 C.: A model for European Biogenic Volatile Organic Compound emissions: Software
1585 development and first validation. Environ. Model. Softw. 25, 1845–1856.
1586 doi:10.1016/j.envsoft.2010.05.004, 2010.

1587 Potempski, S., Galmarini, S., Riccio, A., and Giunta, G.: Bayesian model averaging for
1588 emergency response atmospheric dispersion multimodel ensembles: Is it really better? How
1589 many data are needed? Are the weights portable?, J. Geophys. Res., 115, D21309,
1590 doi:10.1029/2010JD014210, 2010.

1591 Rabitz, H., Ö.F., Alis: General foundations of high-dimensional model representations, J.
1592 Math. Chem., 25, 197-233, 1999.

1593 Rao, S.T., Galmarini, S., and Puckett, K.: Air quality model evaluation international initiative
1594 (AQMEII). Bull. Am. Meteor. Soc., 92, 23-30. DOI:10.1175/2010BAMS3069.1, 2011.

1595 Riccio, A., Giunta, G., and Galmarini, S.: Seeking for the rational basis of the Median Model:
1596 the optimal combination of multi-model ensemble results, Atmos. Chem. Phys., 7, 6085–
1597 6098, doi:10.5194/acp-7-6085-2007, 2007.

1598 Robertson, L., Langner, J. and Engardt, M.: An Eulerian limited-area atmospheric transport
1599 model. J. Appl. Met. 38, 190-210, 1999.

1600 Roselle, S.J., and Binkowski, F.S.: Cloud Dynamics and Chemistry, in: Science algorithms of
1601 the EPA Models-3 Community multiscale air quality (CMAQ) modeling system, EPA 600/R-
1602 99-030, EPA, 1999.

1603 Rouil, L., Honoré, C., Vautard, R., Beekmann, M., Bessagnet, B., Malherbe, L., Meleux, F.,
1604 Dufour, A., Elichegaray, C., Flaud, J.-M., Menut, L., Martin, D., Peuch, A., Peuch, V.-H., and
1605 Poisson, N.: PREV'AIR: an operational forecasting and mapping system for air quality in
1606 Europe, Bull. Am. Meteor. Soc., 90(1), 73-83, doi:10.1175/2008BAMS2390.1, 2009.

1607 Schaap, M., van Loon, M., ten Brink, H. M., Dentener, F. J., and Builtjes, P. J. H.: Secondary
1608 inorganic aerosol simulations for Europe with special attention to nitrate, Atmos. Chem.
1609 Phys., 4, 857–874, doi:10.5194/acp-4-857-2004, 2004.

Schaap, M., Timmermans, R. M. A., Sauter, F. J., Roemer, M., Velders, G. J. M., Boersen, G. A. C., Beck, J. P., and Builtjes, P. J. H.: The LOTOS-EUROS model: description, validation and latest developments, Int. J. Environ. Pollut., 32, 270–289, 2008.

Schaap, M., Manders, A.A.M, Hendriks, E.C.J., Cnossen, J.M., Segers, A.J.S., Denier van der Gon, H.A.C., Jozwicka, M., Sauter, F.J., Velders, G.J.M., Matthijsen, J., Builtjes P.J.H.: Regional modelling of particulate matter for Netherlands' published by the Neterlands Research Programme on particulate matter. Report 500099008, ISSN: 1875-2322 (print) ISSN: 1875-2314. 2005.

Sandu, A., Daescu, D. N., and Carmichael, G.R.: Direct and adjoint sensitivity analysis of chemical kinetic systems with KPP: part I – theory and software Tools, Atmos. Env., 37, 5083-5096, 2003.

Sandu, A., and Sander, R.: Technical node: Simulating chemical systems in Fortran90 and Matlab with the Jinetic PreProcessor KPP-2.1, Atmos. Chem. Phys., 6, 187-195, 2006.

Sič, B., El Amraoui, L., Marécal, V., Josse, B., Arteta, J., Guth, J., Joly, M., and Hamer, P. D.: Modelling of primary aerosols in the chemical transport model MOCAGE: development and evaluation of aerosol physical parameterizations, Geosci. Model Dev., 8, 381–408, doi:10.5194/gmd-8-381-2015, 2015.

Simpson, D., Andersson-Sköld, Y., and Jenkin, M.E.: Updating the chemical scheme for the EMEP MSC-W oxidant model: current status. EMEP MSC-W Nore 2/93, 1993.

Simpson, D., Winiwarter, W., Börjesson, G., Cinderby, S., Ferreiro, A., Guenther, A., Hewitt, C. N., Janson, R., Khalil, M. A. K., Owen, S., Pierce, T. T., Puxbaum, H., Shearer, M., Skiba, U., Steinbrecher, R., Tarrason, L., and Oquist, M. G.: Inventorying emissions from nature in Europe, J. Geophys. Res.: Atmospheres (1984–2012), 104, 8113–8152, 1999.

Simpson, D., Fagerli, H., Jonson, J. E., Tsyro, S., Wind, P., and Tuovinen, J.-P.: Transboundary Acidification, Eutrophication and Ground Level Ozone in Europe, Part 1: Unified EMEP Model Description, EMEP Report 1/2003, 2003.

Simpson, D., Benedictow, A., Berge, H., Bergström, R., Emberson, L. D., Fagerli, H., Flechard, C. R., Hayman, G. D., Gauss, M., Jonson, J. E., Jenkin, M. E., Nyiri, A., Richter, C., Semeena, V. S., Tsyro, S., Tuovinen, J.-P., Valdebenito, A., and Wind, P.: The EMEP MSC-W chemical transport model – technical description, Atmos. Chem. Phys., 12, 7825–7865, 2012.

1641 Skamarock, W.C., Klemp, J.B., Dudhia, J., Gill, D.O., Barker, D.M., Duda, M.G., Huang,
1642 X.Y., Wang, W., Powers, J.G.: A description of the advanced researcher WRF version 3.
1643 NCAR Technical Note, NCAR/TN-475+STR, June 2008, Boulder, Colorado, USA, 125 pp,
1644 2008.

1645 Sofiev, M.: A model for the evaluation of long-term airborne pollution transport at regional
1646 and continental scales. Atmos. Environ. 34, 2481–2493, 2000.

1647 Sofiev, M.: Extended resistance analogy for construction of the vertical diffusion scheme for
1648 dispersion models. J. Geophys. Res. 107. doi:10.1029/2001JD001233, 2002.

1649 Sofiev, M., Galperin, M. V, and Genikhovich, E.: Construction and evaluation of Eulerian
1650 dynamic core for the air quality and emergency modeling system SILAM, in: Borrego, C.,
1651 Miranda, A.I. (Eds.), NATO Science for Piece and Security Serties C: Environmental
1652 Security. Air Pollution Modelling and Its Application, XIX. SPRINGER-VERLAG BERLIN,
1653 pp. 699–701, 2008.

1654 Sofiev, M., Genikhovich, E., Keronen, P., and Vesala, T.: Diagnosing the Surface Layer
1655 Parameters for Dispersion Models within the Meteorological-to-Dispersion Modeling
1656 Interface. J. Appl. Meteorol. Climatol. 49, 221–233. doi:10.1175/2009JAMC2210.1, 2010.

1657 Sofiev, M., Siljamo, P., Valkama, I., Ilvonen, M., and Kukkonen, J.: A dispersion modelling
1658 system SILAM and its evaluation against ETEX data. Atmos. Environ. 40, 674–685.
1659 doi:10.1016/j.atmosenv.2005.09.069, 2006.

1660 Sofiev, M., Soares, J., Prank, M., de Leeuw, G., Kukkonen, J.: A regional-to-global model of
1661 emission and transport of sea salt particles in the atmosphere. J. Geophys. Res. 116.
1662 doi:10.1029/2010JD014713, 2011.

1663 Sofiev. M., Berger, U., Prank, M., Vira, J., Arteta, J., Belmonte, J., Bergmann, K.-C. ,
1664 Cheroux, F., Elbern, H., Friese, E., Galan, C., Gehrig, R., Kranenburg, R., Marécal, V.,
1665 Meleux, F., Pessi, A.-M., Robertson, L., Ritenberga, O., Rodinkova, V. , Saarto, A., Segers,
1666 A., Severova, E., Sauliene, I., Steensen, B. M., Teinemaa, E., Thibaudon, M., and Peuch, V.-
1667 H.: Multi-model simulations of birch pollen in Europe by MACC regional ensemble, Atmos.
1668 Chem. Phys., 15, 8115-8130, 2015.

1669 Solazzo, E., Bianconi, R., Vautard, R., Appel, K. W., Moran, M. D., Hogrefe, C., Bessagnet,
1670 B., Brandt, J., Christensen, J. H., Chemel, C., Coll, I., Denier van der Gon, H., Ferreira, J.,
1671 Forkel, R., Francis, X. V., Grell, 5 G., Grossi, P., Hansen, A. B., Jericevic, A., Kraljevic, L.,

Miranda, A. I., Nopmongcol, U., Pirovano, G., Prank, M., Riccio, A., Sartelet, K. N., Schaap, M., Silver, J. D., Sokhi, R. S., Vira, J., Werhahn, J., Wolke, R., Yarwood, G., Zhang, J., Rao, S. T., and Galmarini, S.: Model eva- lution and ensemble modelling of surface-level ozone in Europe and North America in the context of AQMEII, Atmos. Env., 53, 60–74, 2012a.

Solazzo, E., Bianconi, R., Pirovano, G., Matthias, V., Vautard, R., Moran, M. D., Wyat Appel, K., Bessagnet, B., Brandt, J., Chris- tensen, J. H., Chemel, C., Coll, I., Ferreira, J., Forkel, R., Francis, X. V., Grell, G., Grossi, P., Hansen, A. B., Miranda, A. I., Nop- mongcol, U., Prank, M., Sartelet, K. N., Schaap, M., Silver, J. D., Sokhi, R. S., Vira, J., Werhahn, J., Wolke, R., Yarwood, G., Zhang, J., Rao, S. T., and Galmarini, S.: Operation model evalu- ation for particulate matter in Europe and North America in the context of AQMEII, Atmos. Env., 53, 75–92, 2012b.

Stein, O., Flemming, J., Inness, A., Kaiser, J. W., and Schultz, M. G.: Global reactive gases and reanalysis in the MACC project, Journal of Integrative Environmental Sciences, 9, Iss. sup1, 57– 70, doi:10.1080/1943815X.2012.696545, 2012.

Stern, R., Builtjes, P., Schaap, M., Timmermans, R. M. A., Vautard, R., Hodzic, A., Memmesheimer, M., Feldmann, H., Renner, E., Wolke, R., and Kerschbaumer, A.: A model inter-comparison study focussing on episodes with elevated PM10 concentrations, Atmos. Env., 42, 4567-4588, 10.1016/j.atmosenv.2008.01.068, 2008.

Stockwell, W. R., Kirchner, F., Kuhn, M., and Seefeld, S.: A new mechanism for regional atmospheric chemistry modeling, J. Geophys. Res. : Atmospheres, 102, 25 847–25 879, 1997.

Tie, X., Madronich, S., Walters, S., Zhang, R., Rasch, P., and Collins, W.: Effect of clouds on photolysis and oxidants in the troposphere, J. Geophys. Res., 108 (D20), 4642, doi : 10.1029/2003JD003659, 2003.

Timmermans, R.M.A., Schaap, M., Elbern, H., Siddans, R., Tjemkes, S.A.T., Vautard, R., and Builtjes, P.J.H.: An Observing System Simulation Experiment (OSSE) for Aerosol Optical Depth from satellites, J. Atmos. Ocean. Technol., 26, 2673-2682, 2009.

Tuovinen, J.-P., Ashmore, M., Emberson, L., and Simpson, D.: Testing and improving the EMEP ozone deposition module, Atmos. Env., 38, 2373–2385, 2004.

Turquety, S., Menut, L., Bessagnet, B., Anav, A., Viovy, N., Maignan, F., and Wooste, M.: APIFLAME v1.0: high-resolution fire emission model and application to the Euro Mediterranean region, Geosci. Model Dev., 7, 587–612, 2014.

1703 Van Loon, M., Vautard, R., Schaap, M., Bergstrom, R., Bessagnet, B., Brandtn J., Builtjes,
1704 P.J.H, Christensen, J.H., Cuvelier, C., Graff, A., Jonson, J.E., Krol, M., Langner, J., Roberts,
1705 P., Rouil, L., Stern, R., Tarrason, L., Thunis, P., Vignati, E., and White, L.: Evaluation of
1706 long-term ozone simulations from seven regional air quality models and their ensemble,
1707 Atmos. Env., 41, 2083-2097, 10.1016/j.atmosenv.2006.10.073, 2007.

1708 Van Ulden, A.P, and Holtslag, A.A.M.: Estimation of atmospheric boundary layer parameters
1709 fort diffusion applications, J. Climate. Appl. Met., 24, 1196-1207, 1975.

1710 Vautard, R. , Builtjes, P.H.J., Thunis,P., C. Cuvelier,Bedogni,M., Bessagnet, B., Honoré, C.,
1711 Moussiopoulos, N., Pirovano, G., Schaap, M., Stern, R., Tarrason, L., and Wind,
1712 P.:Evaluation and intercomparison of Ozone and PM10 simulations by several chemistry
1713 transport models over four European cities within the CityDelta project, Atmos. Env. , 41,
1714 173–188, 2007.

1715 Vira, J., and Sofiev, M.:On variational data assimilation for estimating the model initial
1716 conditions and emission fluxes for short-term forecasting of SOx concentrations. Atmos.
1717 Env., 46, 318–328. doi:10.1016/j.atmosenv.2011.09.066, 2012.

1718 Vira, J. and Sofiev, M.: Assimilation of surface NO2 and O3 observations into the SILAM
1719 chemistry transport model, Geosci. Model Dev., 8, 191–203, doi:10.5194/gmd-8-191-2015,
1720 2015.

1721 Visschedijk, A. J. H., Zandveld, P. Y. J., and Denier van der Gon, H. A. C. A.: High
1722 resolution gridded European database for the EU Integrate Project GEMS, TNO-report 2007-
1723 A-R0233/B, 2007.

1724 Walcek, C.J.: Minor flux adjustment near mixing ratio extremes for simplified yet highly
1725 accurate monotonic calculation of tracer advection, J. Geophy. Res., 105(D7), 9335-9348,
1726 2000.

1727 Wichink Kruit, R. J., Schaap, M., Sauter, F. J., van Zanten, M. C., and van Pul, W. A. J.:
1728 Modeling the distribution of ammonia across Europe including bi-directional surface–
1729 atmosphere ex- change, Biogeosciences, 9, 5261–5277, doi:10.5194/bg-9-5261- 2012, 2012.

1730 Vlemmix, T., Eskes, H. J., Piters, A. J. M., Schaap, M., Sauter, F. J., Kelder, H., and Levelt,
1731 P. F., MAX-DOAS tropospheric nitrogen dioxide column measurements compared with the
1732 Lotos-Euros air quality model, Atmos. Chem. Phys., 15, 1313-1330, doi:10.5194/acp-15-
1733 1313-2015, 2015.

1734 Weaver, A., and Courtier, P.: Correlation modeling on the sphere using a generalized
1735 diffusion equation, Q. J. R. Meteorol. Soc., 127, 1815-1846, 2001.

1736 Wesely, M.: Parameterization of surface resistances to gaseous dry deposition in regional-
1737 scale numerical models, Atmos. Env. (1967), 23, 1293 – 1304, 1989.

1738 Williams, J. E., van Velthoven, P. F. J., and Brenninkmeijer, C. A. M.: Quantifying the
1739 uncertainty in simulating global tropospheric composition due to the variability in global
1740 emission estimates of Biogenic Volatile Organic Compounds, Atmos. Chem. Phys., 13, 2857-
1741 2891, doi:10.5194/acp-13-2857-2013, 2013.

1742 Williamson, D.L., and Rasch, R. P.: Two-Dimensional Semi-Lagrangian Transport with
1743 Shape-Preserving Interpolation, American Meteorological Society, 117, 102–129, 1989.

1744 WHO (World Health Organization): Health aspects of air pollution results from the WHO
1745 project “Systematic review of health aspects of air pollution in Europe”, Technical Report,
1746 2004.

1747 WHO (World Health Organization): Review of evidence on health aspects of air pollution –
1748 REVIHAAP Project, Technical Report, 2013.

1749 Yarwood, G., Rao, S., Yocke, M., and Whitten, G.Z.: Updates to the carbon bond chemical
1750 mechanism: CB05, Report to the U.S. Environmental Protection Agency, RT-04-00675,
1751 Yocke and Company, Novato, California, United States, 2005.

1752 Zhang, L., Brook, J.R., and Vet, R.: A revised parameterization for gaseous dry deposition in
1753 air-quality models, Atmos. Chem. Phys., 3, 2067-2082, 2003.

1754 Zhang, L, Gong, S., Padro, J., and Barrie, L.: A size-segregated particle dry deposition
1755 scheme for an atmospheric aerosol module. Atmos. Env., 35(3), 2001, 549–560, 2001.

1756 Zhang, Y., Bocquet, M., Mallet, V., Seigneur, C., and Baklanov, A.: Real-time air quality
1757 forecasting, part I: History, techniques, and current status, Atmos. Environ., 60, 632–655,
1758 2012.

1759 Zilitinkevich, S. and Mornom, D.V.: A multi-limit formulation for the equilibrium depth of a
1760 stable stratified boundary layer. Max-Planck-Institute for Meteorology. Report No. 185, ISSN
1761 0397-1060, 30 pp., 1996.

1762 Zyryanov, D., Foret, G., Eremenko, M., Beekmann, M., Cammas, J.-P., D'Isidoro, M., Elbern,
1763 H., Flemming, J., Friese, E., Kioutsioutkis, I., Maurizi, A., Melas, D., Meleux, F., Menut, L.,

1764 Moinat, P., Peuch, V.-H., Poupkou, A., Razinger, M., Schultz, M., Stein, O., Suttie, A. M.,
1765 Valdebenito, A., Zerefos, C., Dufour, G., Bergametti, G., and Flaud, J.-M.: 3-D evaluation of
1766 tropospheric ozone simulations by an ensemble of regional Chemistry Transport Models,
1767 Atmos. Chem. Phys., 12, 3219-3240, 2012, doi:10.5194/acp-12-3219-2012.

1768

1769

1770 Table 1. Portfolio of the MACC-II regional data products. Each product is provided once
1771 daily. Core species correspond to O_3, NO_2, CO, SO_2, PM10, PM2.5. Additional species
1772 correspond to NO, NH_3, PAN+PAN precursors, total Non-Methane Volatile Organic
1773 Compounds. Birch pollen concentrations are only available during season from 1st of March
1774 to 30th of June each year. Old levels refer to surface, 500m, 1000m, 3000m and 5000m,
1775 corresponding to the production before mid-May 2014. All levels refers to surface, 50m,
1776 250m, 500m, 1000m, 2000m, 3000m and 5000m, produced from mid-May 2014. The analysis
1777 is run *a posteriori* on Day0 for Day-1 (00 to 24UTC).

Model name	Forecast or Analysis	Species	Time span	Vertical levels	Format
CHIMERE	Forecast	core + additional	0h to 96h, hourly	All levels	Netcdf
CHIMERE	Forecast	Birch pollen	0h to 96h, hourly	Surface	Netcdf
CHIMERE	Analysis	O_3 , PM10	-24h to -1h, hourly	Surface	Netcdf
EMEP	Forecast	core + additional	0h to 96h, hourly	All levels	Netcdf
EMEP	Forecast	Birch pollen	0h to 96h, hourly	Surface	Netcdf
EMEP	Analysis	NO_2	-24h to -1h, hourly	Surface	Netcdf
EURAD-IM	Forecast	core + additional	0h to 96h, hourly	All levels	Netcdf
EURAD-IM	Forecast	Birch pollen	0h to 96h, hourly	Surface	Netcdf
EURAD-IM	Analysis	O_3, NO_2, CO, SO_2, PM10	-24h to -1h, hourly	Surface	Netcdf
LOTOS-EUROS	Forecast	core + NO	0h to 96h, hourly	Old levels	Netcdf

LOTOS-EUROS	Forecast	Birch pollen	0h to 96h, hourly	Surface	Netcdf
LOTOS-EUROS	Analysis	O_3	-24h to -1h, hourly	Surface	Netcdf
MATCH	Forecast	core + additional	0h to 96h, hourly	All levels	Netcdf
MATCH	Forecast	Birch pollen	0h to 96h, hourly	Surface	Netcdf
MATCH	Analysis	O_3, NO_2, CO,PM10, PM2.5	-24h to -1h, hourly	Surface	Netcdf
MOCAGE	Forecast	core + additional (except NH_3)	0h to 96h, hourly	All levels	Netcdf
MOCAGE	Forecast	Birch pollen	0h to 96h, hourly	Surface	Netcdf
MOCAGE	Analysis	O_3	-24h to -1h, hourly	Surface	Netcdf
SILAM	Forecast	core	0h to 96h, hourly	All levels	Netcdf
SILAM	Forecast	Birch pollen	0h to 96h, hourly	Surface	Netcdf
SILAM	Analysis	O_3, NO_2, SO_2	-24h to -1h, hourly	Surface	Netcdf
ENSEMBLE	Forecast	core + additional	0h to 96h, hourly	All levels	Netcdf + Grib2
ENSEMBLE	Forecast	Birch pollen	0h to 96h, hourly	Surface	Netcdf + Grib2
ENSEMBLE	Analysis	O_3	-24h to -1h,	Surface	Netcdf +

		hourly	Grib2

1781 Table 2. Time of delivery of the ENSEMBLE numerical products. Core species for the
1782 analysis is restricted to ozone only.

	Forecast Day0 (0h-24h)	Forecast Day1 (25h-48h)	Forecast Day2 (49h-72h)	Forecast Day3 (73h-96h)	Analysis (-24h-0h)
Core species	07 UTC	07 UTC	08 UTC	09 UTC	14:30 UTC
Additional species	07 UTC	07 UTC	08 UTC	09 UTC	N/A

1783

1784

1785 Table 3. General characteristics of the regional models at the end of MACC-II project.

Model	Operated by	Horizontal resolution	Vertical levels Top height
CHIMERE	INERIS (Institut National de l'Environnement Industriel et des Risques) France	0.1° x 0.1°	8 levels Top at 500 hPa
EMEP	MET Norway (Meteorologisk institutt) Norway	0.25° x 0.125°	20 levels top at 100 hPa
EURAD-IM	RIUUK (Rheinisches Institut Fuer Umwelt-Forschung an der Universitaet zu Koeln E. V.) Germany	15 km on a Lambert conformal projection	23 levels Top at 100 hPa
LOTOS-EUROS	KNMI (Koninklijk Nederlands Meteorologisch Instituut) Netherlands	0.25° x 0.125°	4 levels Top at 3.5km
MATCH	SMHI (Sveriges Meteorologiska och Hydrologiska Institut) Sweden	0.2° x 0.2°	52 levels Top at 300 hPa
MOCAGE	Météo-France France	0.2° x 0.2°	47 levels Top at 5 hPa
SILAM	FMI (Ilmatieteen Laitos) Finland	0.15° x 0.15°	8 levels Top at 6.7 km

1786

1787

1788 Table 4. Characteristics of the daily assimilation chains of the regional models at the end of
1789 MACC-II project.

Model	Assimilation method	Observation assimilated	Species analysed
CHIMERE	Optimal interpolation	O_3 and PM_{10} from surface stations,	O_3, PM_{10}
EMEP	3D- Variational	NO_2 columns from OMI and NO_2 from surface stations	NO_2
EURAD-IM	3D- Variational	O_3, NO, NO_2, SO_2, CO, PM_{10}, $PM_{2.5}$ from surface stations, OMI and GOME-2 NO_2 column retrievals, MOPITT CO profiles	O_3, NO_2, SO_2, CO, PM_{10}
LOTOS-EUROS	Ensemble Kalman filter	O_3 from surface stations	O_3
MATCH	3D- Variational	O_3, NO_2, CO, PM_{10}, $PM_{2.5}$ from surface stations	O_3, NO_2, CO, PM_{10}, $PM_{2.5}$
MOCAGE	3D- Variational	O_3 from surface stations	O_3
SILAM	4D-Variational	O_3, NO_2 and SO_2 from surface stations	O_3, NO_2, SO_2

1790

1791

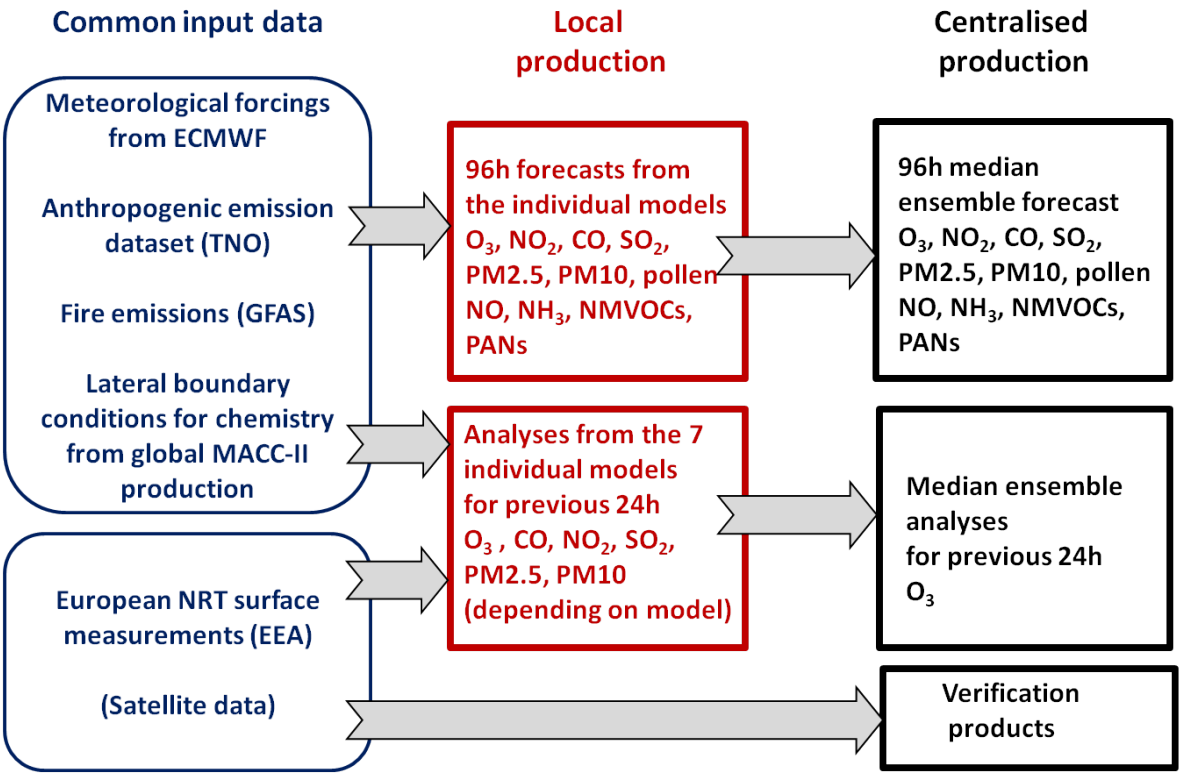

1792

1793

1794 Figure 1. Schematic of the general organisation of the MACC-II air quality forecast and

1795 analysis system.

1796

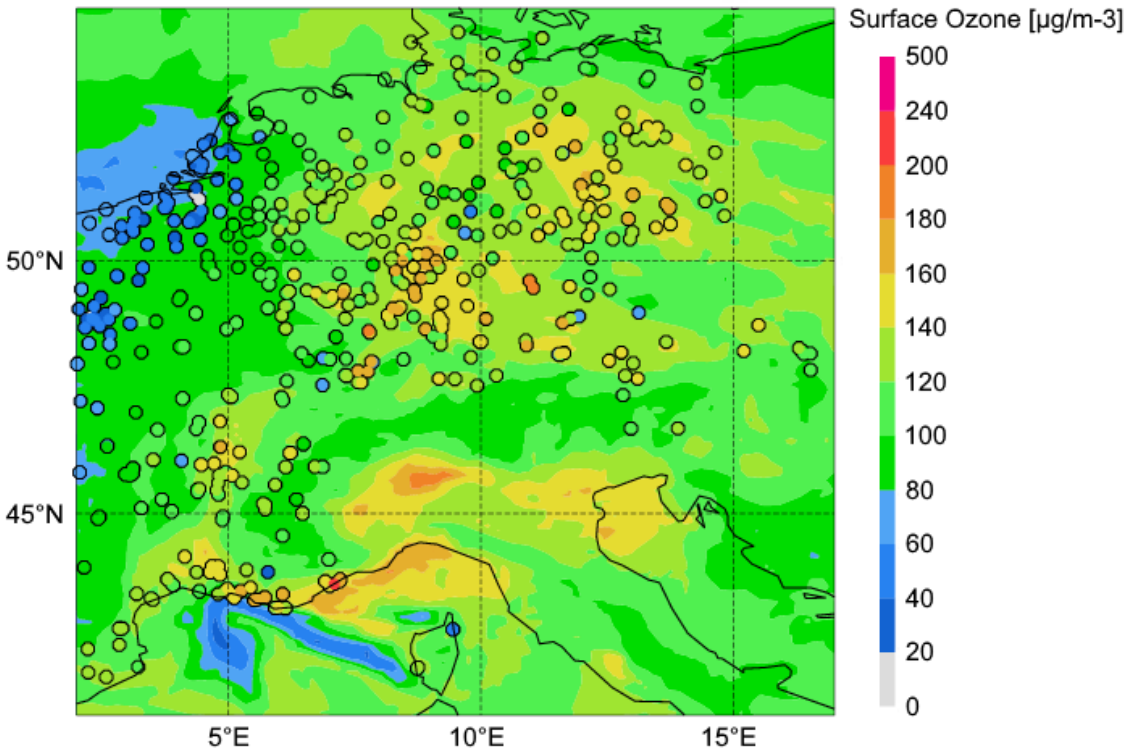

Figure 2. Zoomed map of ozone concentrations at the surface in µg m^{-3} of the 15h forecast for the 10th of June 2014 at 15 UTC of the ensemble median constructed with the 7 model forecasts. NRT AQ observations available (circles) for the same date/time are overpoltted on the maps using the same colour scale.

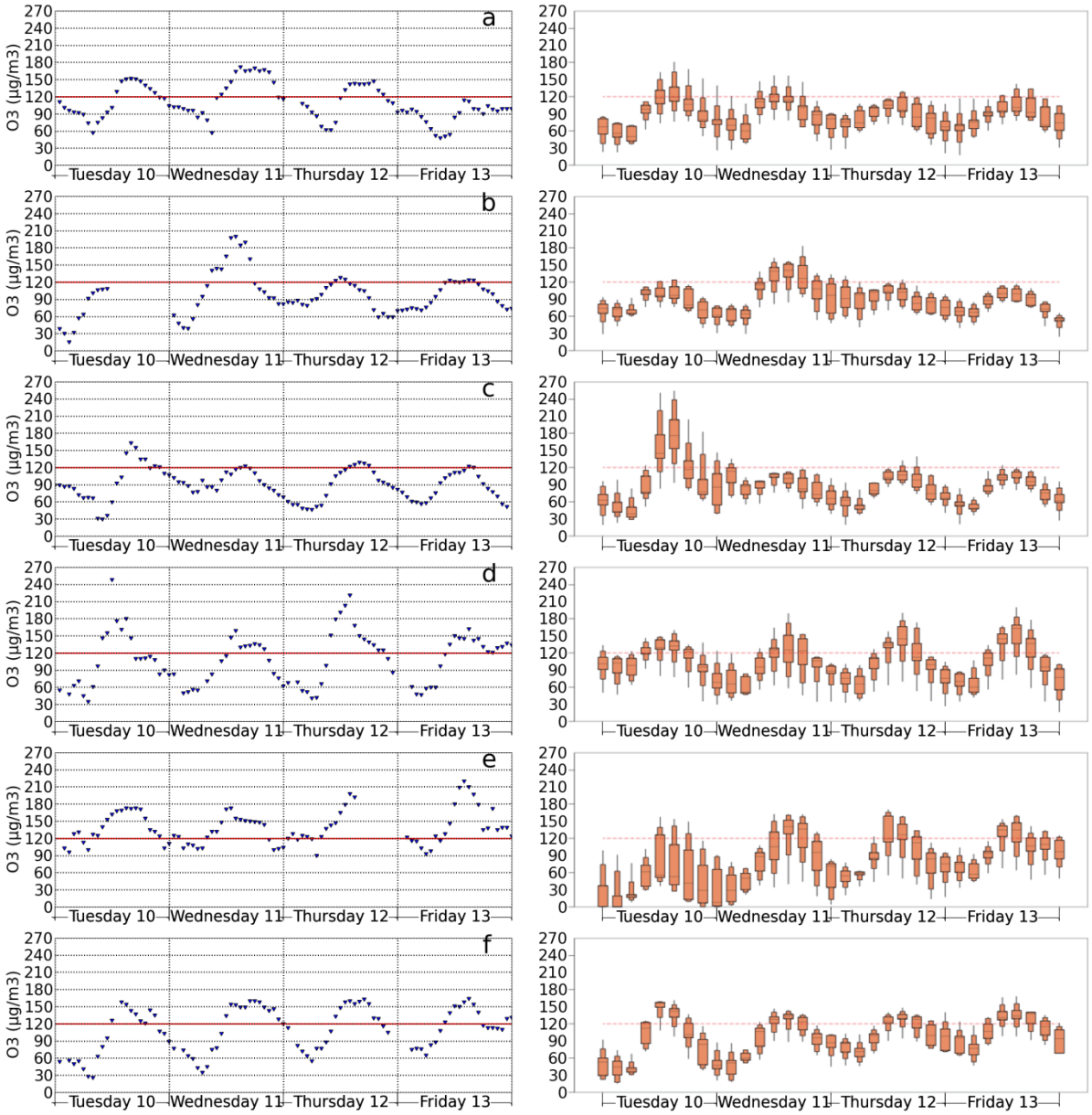

Figure 3. Left panel: Ozone measurements from surface stations in µg m^{-3} from the 10th of June 2014 at 00UTC to the 14th of June 2014 at 00 UTC located (a) at 47.67°N/13.11°E (Hallein, Austria), (b) at 47.69°N/16.58°E (Sopron, Hungaria), (c) at 50.13°N/8.75°E (Fechenheim, Germany), (d) at 43.33°N/5.12°E (Sausset, France), (e) at 43.34°N/5.73°E (Plan d'Aups, France) and (f) at 43.79°N/4.83°E (St Rémi, France). Right panel: EPSgrams giving median, 90% percentile, 75% percentile, 25% percentile, 10% percentile, minimum and maximum from 3-hourly outputs of the 96h forecasts of the 7 models from the 10th of June 2014 at 00UTC to the 14th of June 2014 at 00 UTC. Model outputs are interpolated at the location of the stations shown in the left panel. The red dashed line corresponds to 120 µg m^{-3}.

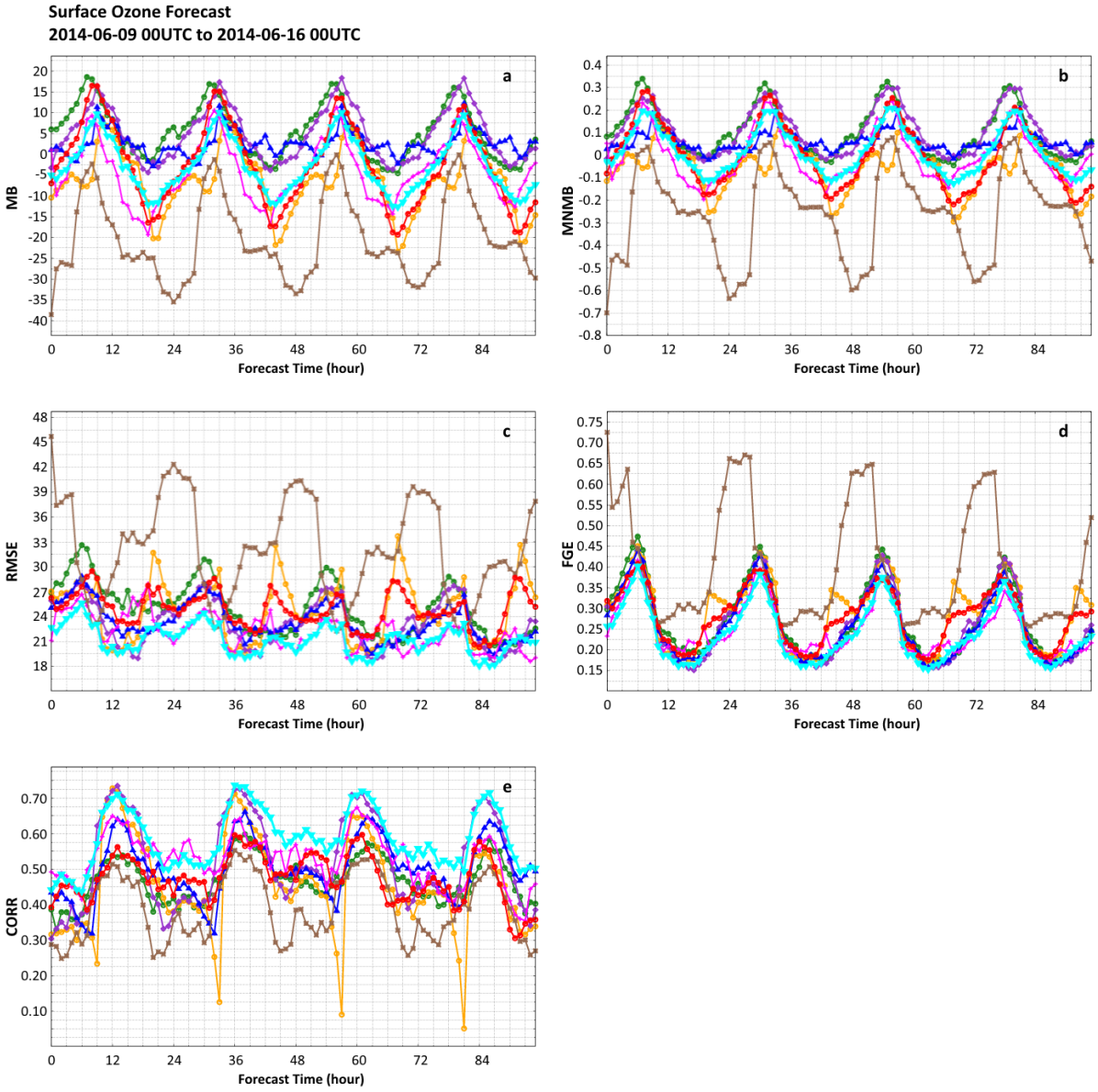

Figure 4. Statistical indicators (see Appendix) for ozone as a function of the forecast time in hour for the ensemble median (in turquoise) and the seven models (other colours) compared to the hourly surface station measurements available for the period from the 9th to the 15th of June 2014 over the MACC-II European domain. (a) MB in μg m^{-3}, (b) MNMB, (c) RMSE in μg m^{-3}, (d) FGE and (e) correlation.

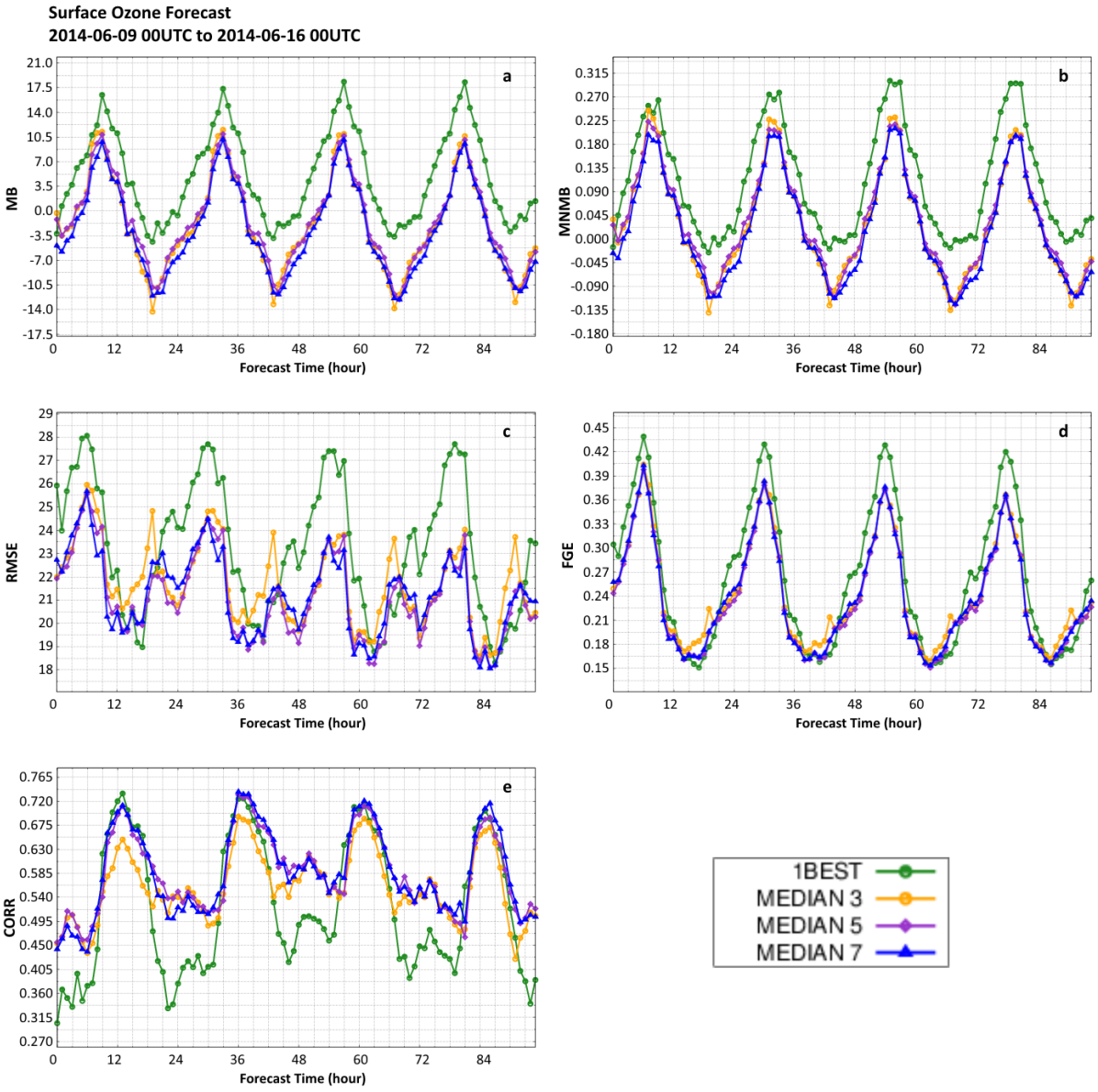

Figure 5. Statistical indicators (see Appendix) for ozone as a function of the forecast time in hour MEDIAN 7, MEDIAN 5, MEDIAN 3 and 1BEST (see text for their definition) compared to the hourly surface station measurements available for the period from the 9th to the 15th of June 2014 over the MACC-II European domain. (a) MB in μg m^{-3}, (b) MNMB, (c) RMSE in μg m^{-3}, (d) FGE and (e) correlation.

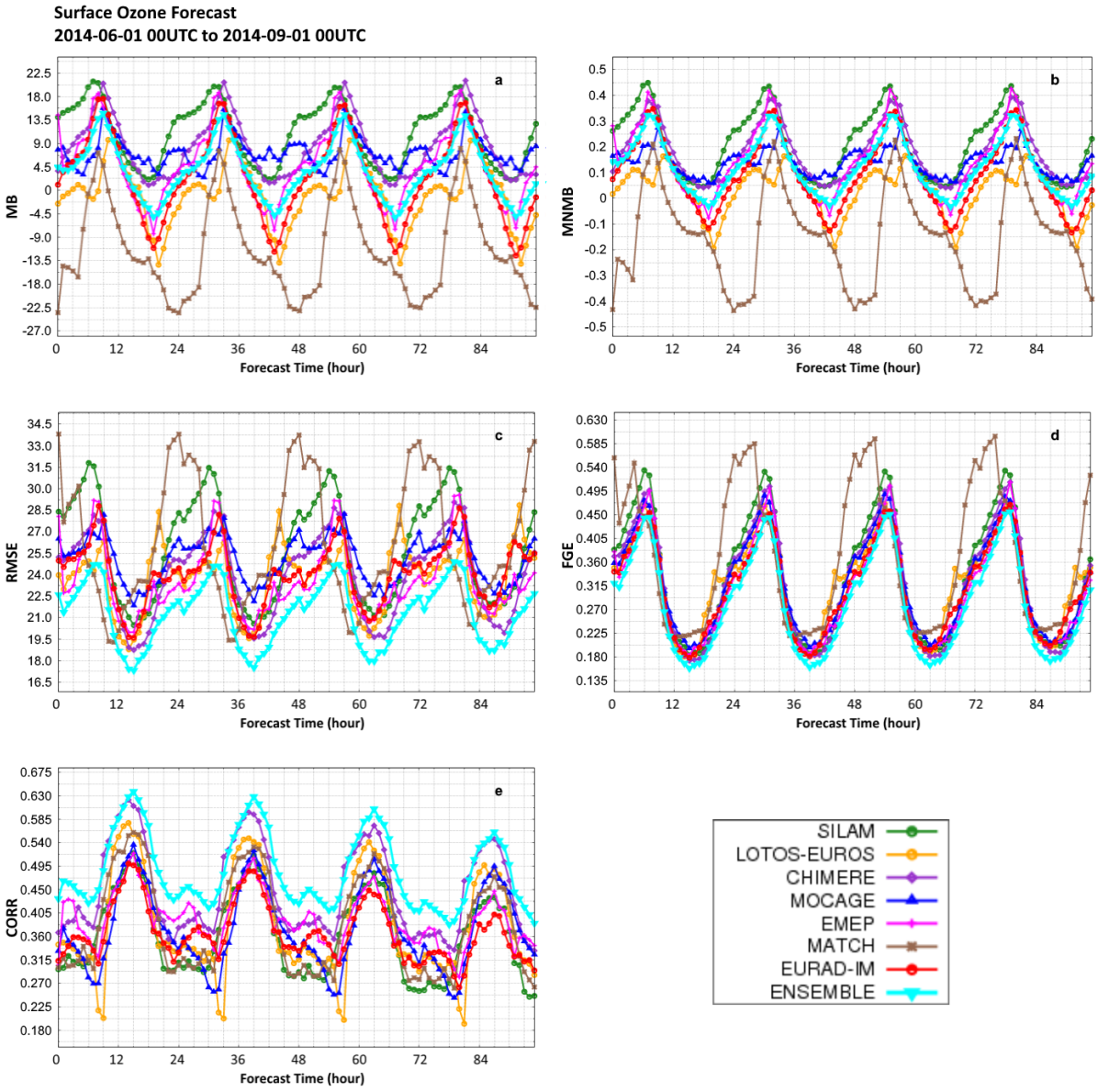

Figure 6. Statistical indicators (see Appendix) for ozone as a function of the forecast time in hour for the ensemble median compared to the hourly surface station measurements available for the period from the 1st of June at 00UTC to the 1st of September at 00UTC over the MACC-II European domain for 2014: (a) MB in μg m^{-3}, (b) MNMB, (c) RMSE in μg m^{-3}, (d) FGE and (e) correlation.

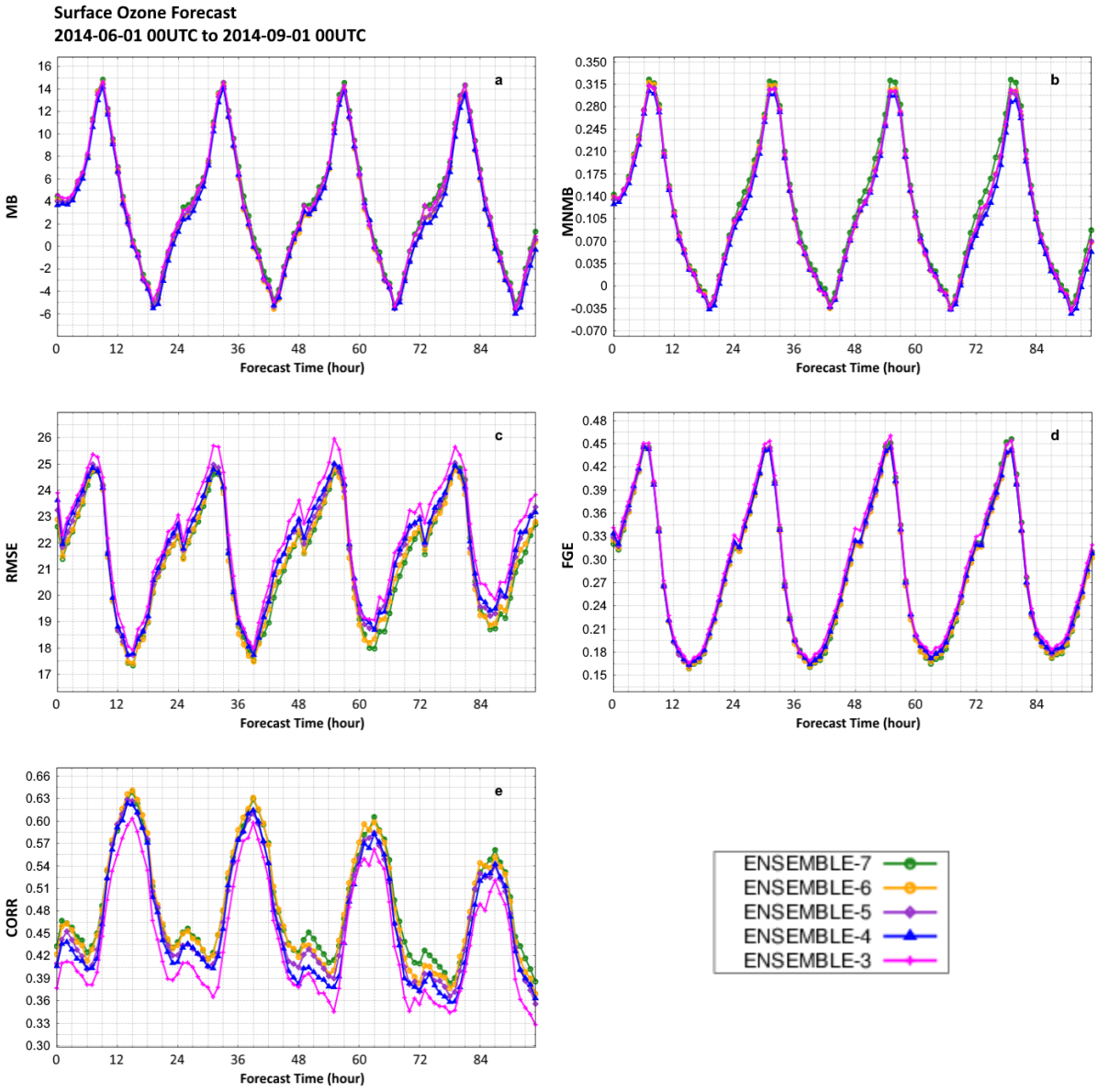

1841

1842 Figure 7. Statistical indicators (see Appendix) for ozone as a function of the forecast time in hour
1843 for an ensemble of 7, 6, 5, 4 and 3 models compared to the hourly surface station measurements
1844 available for the period from the 1st of June 2014 at 00UTC to the 1st of September 2014 at
1845 00UTC over the MACC-II European domain: (a) MB in μg m^{-3}, (b) MNMB, (c) RMSE in μg m^{-3}, (d) FGE and (e) correlation.

1847

1848

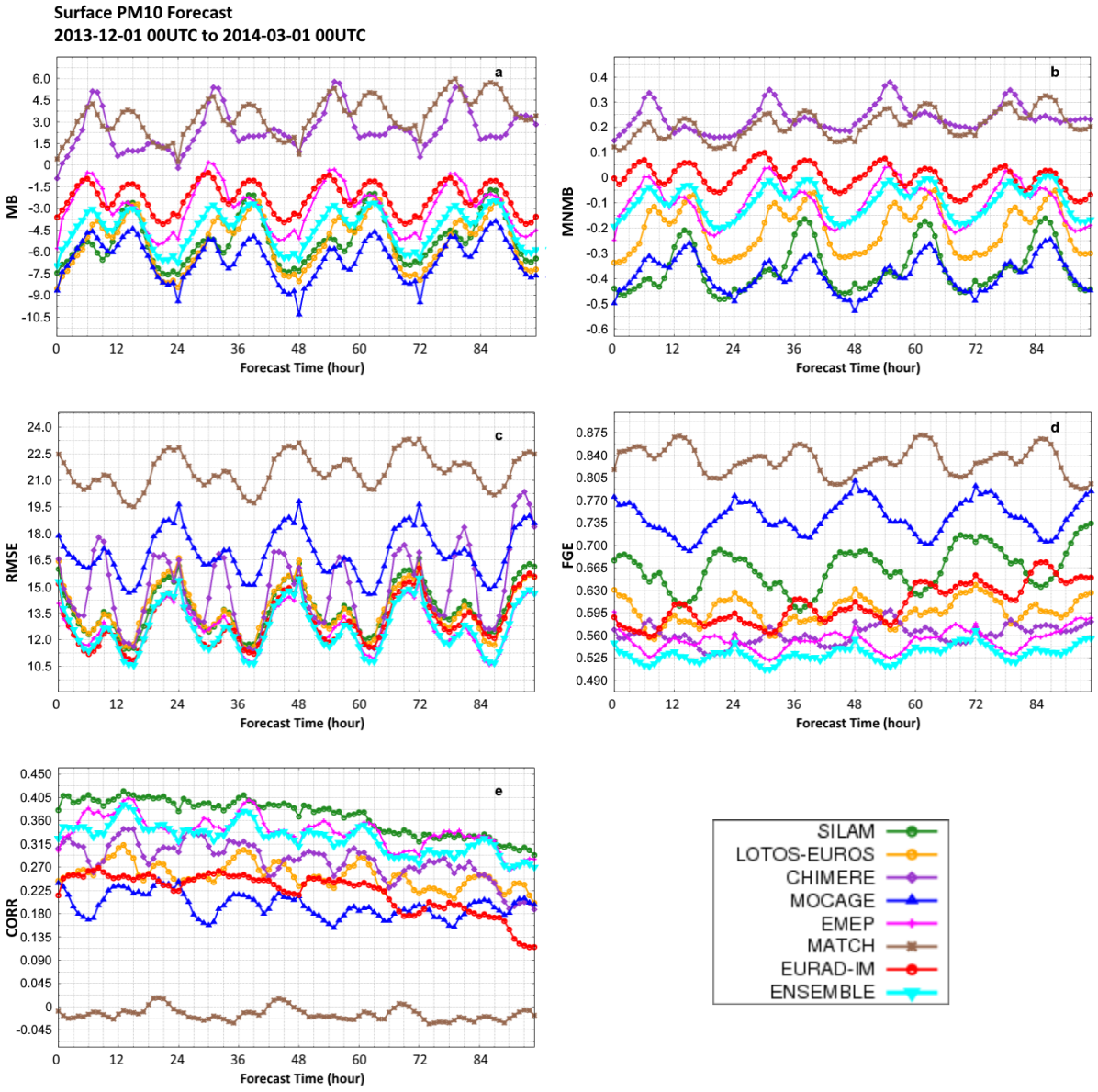

Figure 8. Statistical indicators (see Appendix) for PM_{10} as a function of the forecast time in hour for the ensemble median compared to the hourly surface station measurements available for the period from the 1st of December 2013 at 00UTC to the 1st of March 2014 at 00UTC over the MACC-II European domain: (a) MB in μg m^{-3}, (b) MNMB, (c) RMSE in μg m^{-3}, (d) FGE and (e) correlation.

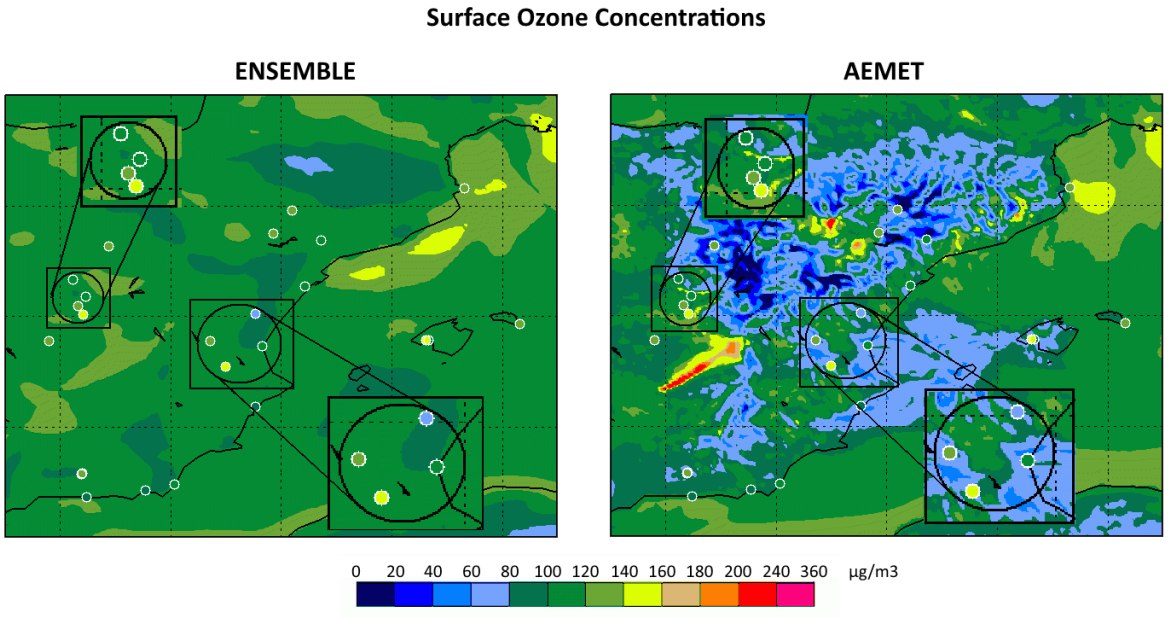

1856

1857

1858 Figure 9. ENSEMBLE (left) and AEMET (right) surface ozone concentrations in µg m^{-3} from
1859 a forecast (H+18) started on 18th July 2013 at 00UTC for the Western Mediterranean area.
1860 Observations from different air quality networks have been plotted on the map. The Madrid
1861 and the Eastern Spain areas appear magnified.

1862

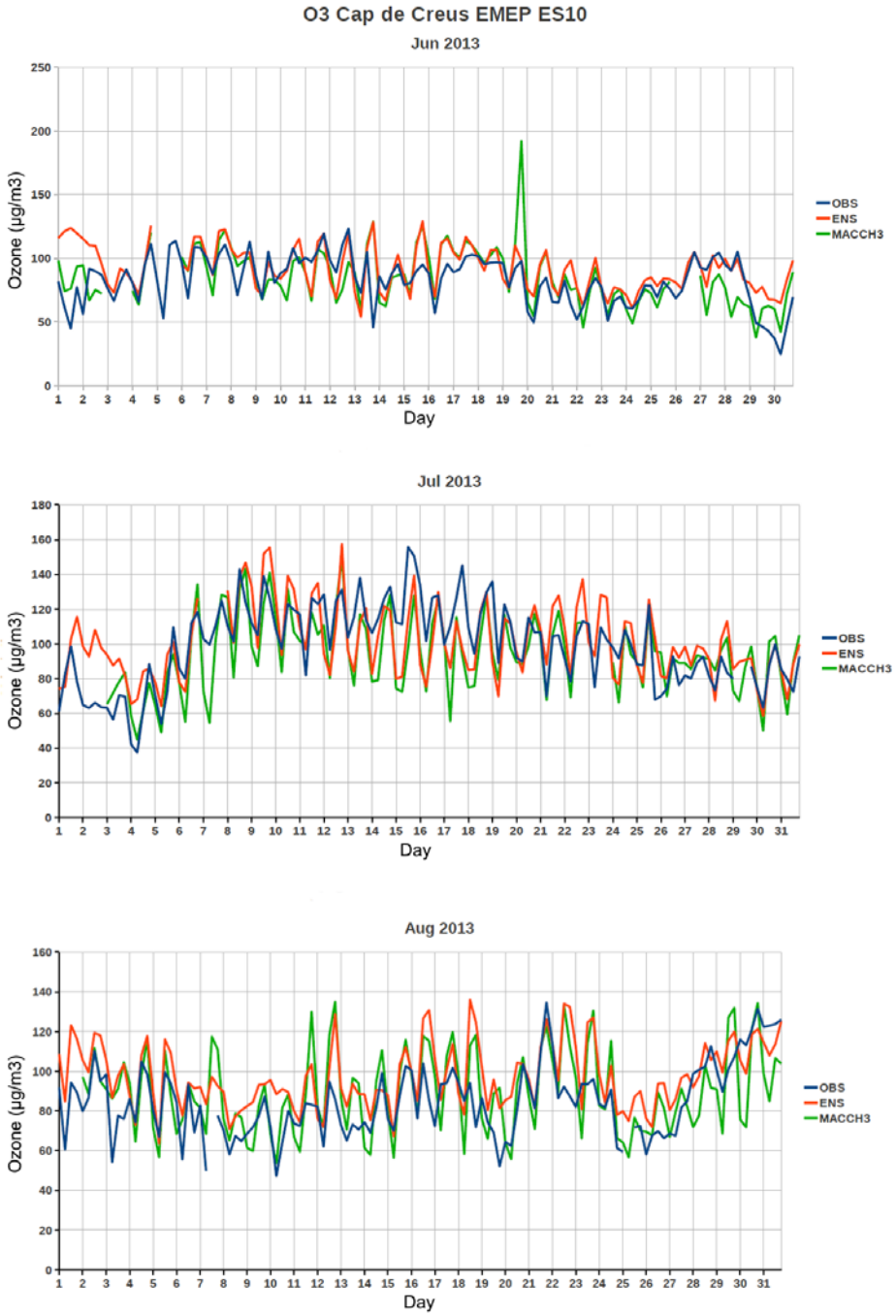

Figure 10. Ozone concentrations in µg m-3 as a function of days at Cap de Creus (42.32°N, 3.32°W). (Top panel) for June 2013, (middle panel) for July 2013 and (bottom panel) for August 2013. The blue colour line is for EMEP observations, the red colour line is for the ENSEMBLE and the green colour line for the AEMET model.

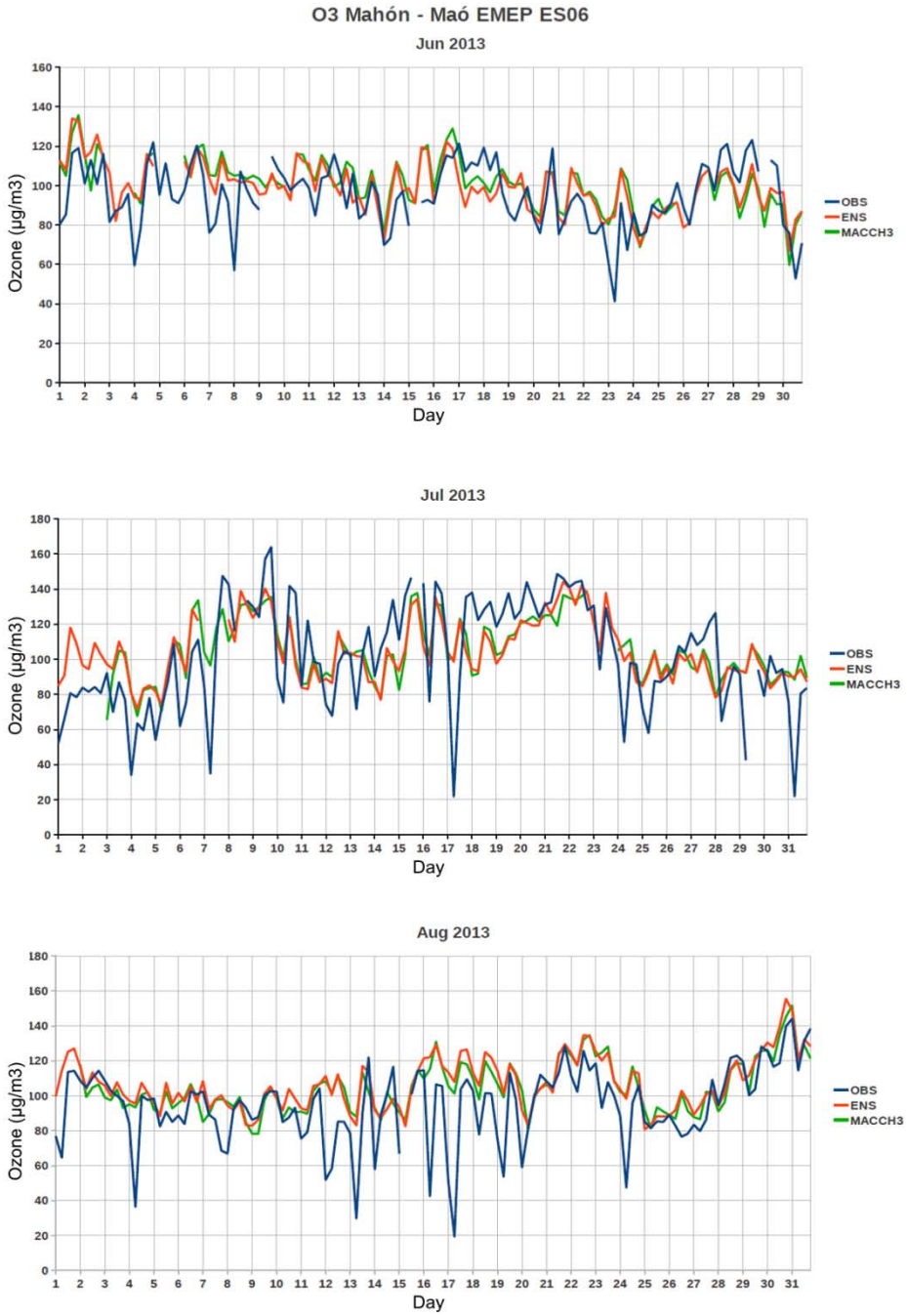

Figure 11. As figure 10 but for Mahon (39.867°N, 4.32°W).

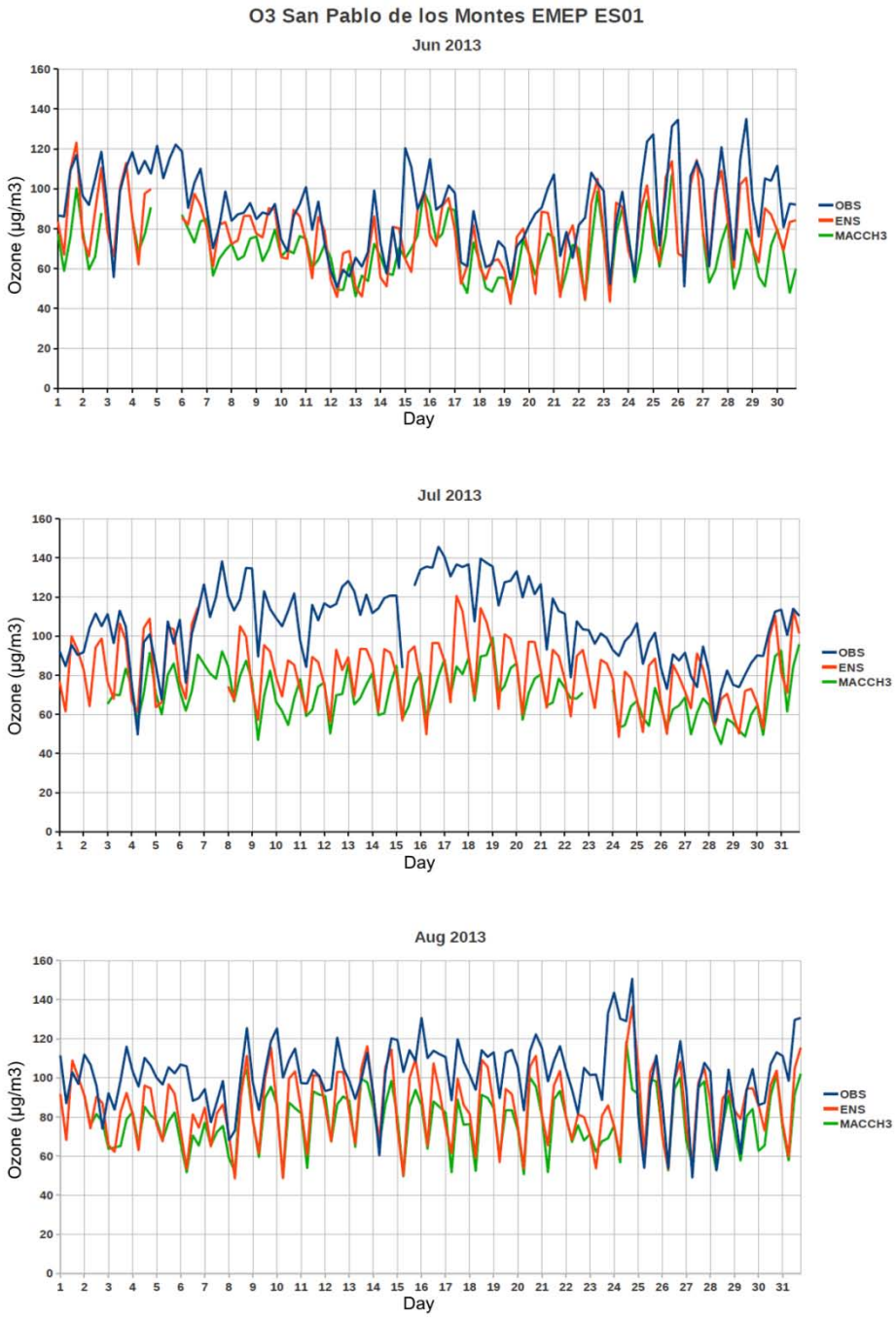

Figure 12. As figure 12 but for San Pablo de los Montes (39.55°N, 4.35°E).

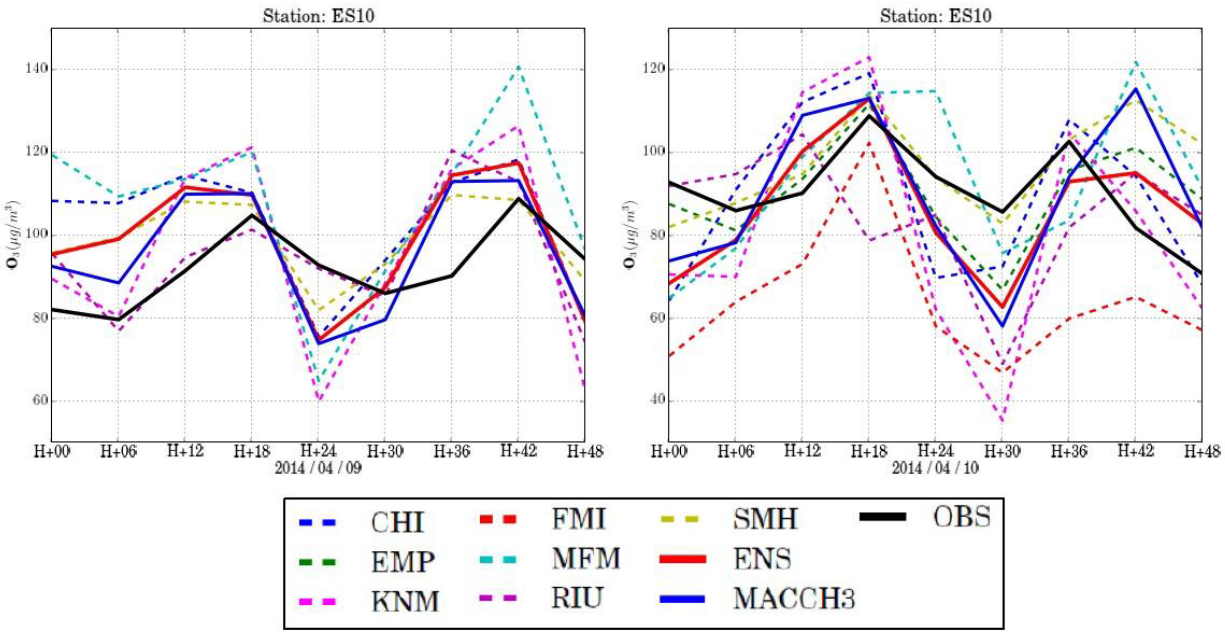

Figure 13. Ozone concentrations (in μg m^{-3}) from a 48h forecast of ENSEMBLE, AEMET and the 7 individual models at ES10 EMEP air quality station which is located at Cabo de Creus in the Northeastern corner of Spain (42.32°N, 3.32°E). The forecast is started on the 9th of April 2014. CHI, EMP, KNM, FMI, MFM, RIU, SMH, ENS, MACCH3 and OBS correspond to CHIMERE, EMEP, LOTOS-EUROS, SILAM, MOCAGE, EURAD-IM, MATCH, ENSEMBLE, AEMET models and observations, respectively.